

10. South, T. L., Blake, P. R., Hare, D. R. & Summers, M. F. C-terminal retroviral-type zinc finger domain from the HIV-1 nucleocapsid protein is structurally similar to the N-terminal zinc finger domain. *Biochemistry* **30**, 6342–6349 (1991).
11. Luisi, B. F. *et al.* Crystallographic analysis of the interaction of the glucocorticoid receptor with DNA. *Nature* **352**, 497–505 (1991).
12. Marmorstein, R., Carey, M., Ptashne, M. & Harrison, S. C. DNA recognition by GAL4: structure of a protein–DNA complex. *Nature* **356**, 408–414 (1992).
13. Everett, R. D. *et al.* A novel arrangement of zinc-binding residues and secondary structure in the C3HC4 motif of an alpha herpes virus protein family. *J. Mol. Biol.* **234**, 1038–1047 (1993).
14. Barlow, P. N., Luisi, B., Milner, A., Elliot, M. & Everett, R. Structure of the C<sub>3</sub>HC<sub>4</sub> domain by <sup>1</sup>H-nuclear magnetic resonance spectroscopy. *J. Mol. Biol.* **237**, 201–211 (1994).
15. Borden, K. L. B. *et al.* The solution structure of the RING finger domain from the acute promyelocytic leukaemia proto-oncoprotein PML. *EMBO J.* **14**, 1532–1541 (1995).
16. Phillips, S. E. V. The β-ribbon DNA recognition motif. *Ann. Rev. Biophys. Biomol. Struct.* **23**, 671–701 (1994).
17. Kim, J. L., Nikolov, D. B. & Burley, S. K. Co-crystal structure of TBP recognizing the minor groove of a TATA element. *Nature* **365**, 520–527 (1993).
18. Kim, Y., Geiger, J. H., Hahn, S. & Sigler, P. B. Crystal structure of a yeast TBP–TATA-box complex. *Nature* **365**, 512–520 (1993).
19. Schumacher, M. A., Choi, K. Y., Zalkin, H. & Brennan, R. G. Crystal structure of LacI member, PurR, bound to DNA: minor groove binding by α-helices. *Science* **266**, 763–770 (1994).
20. Flick, K. E. *et al.* Crystallization and preliminary X-ray studies of I-Ppol: a nuclear, intron-encoded homing endonuclease from *Physarum polycephalum*. *Protein Sci.* **6**, 1–4 (1997).
21. Otwinowski, Z. & Minor, W. Processing of X-ray diffraction data collected in oscillation mode. *Methods Enzymol.* **276**, 307–326 (1997).
22. Leslie, A. G. W. in *Joint CCP4 and ESF-EACMB Newsletter on Protein Crystallography* (Daresbury Laboratory, Warrington, UK, 1992).
23. CCP4 *The SERC (UK) Collaborative Computing Project No. 4, a Suite of Programs for Protein Crystallography* (Daresbury Laboratory, Warrington, UK, 1979).
24. QUANTA96 *X-ray Structure Analysis User's Reference* (Molecular Simulations, San Diego, 1996).
25. Brünger, A. *XPLOR version 3.1: A System for X-ray Crystallography and NMR* (Yale Univ. Press, New Haven, CT, 1992).
26. Laskowski, R. J., MacArthur, M. W., Moss, D. S. & Thornton, J. M. PROCHECK: a program to check the stereochemical quality of protein structures. *J. Appl. Crystallogr.* **26**, 383–290 (1993).
27. Evans, S. V. SETOR: hardware-lighted three-dimensional solid model representations of macromolecules. *J. Mol. Graphics* **11**, 134–138 (1993).

**Acknowledgements.** We thank D. McHugh, K. Stephens and J. D. Heath for initial subcloning, purification and crystallization studies; R. Strong, K. Zhang and B. Scott for advice during the crystallographic analysis; and the beamline staff at the Advanced Light Source (NLBL laboratories), beamline 5.0.2, particularly T. Earnest, for assistance. B.L.S. and R.J.M. are funded for this project by the NIH. K.E.F. was supported by a NIH training grant and the American Heart Association. M.S.J. was supported by an NSF fellowship and an NIH training grant.

Correspondence and requests for materials and coordinates should be addressed to B.L.S. (e-mail: bstoddar@fred.hcr.org). Coordinates have been deposited in the Brookhaven Protein Data Bank (accession nos lipp, 1a73, 1a74).

## corrections

# Emergence of symbiosis in peptide self-replication through a hypercyclic network

David H. Lee, Kay Severin, Yohei Yokobayashi & M. Reza Ghadiri

*Nature* **390**, 591–594 (1997)

Hypercycles are based on second-order (or higher) autocatalysis and defined by two or more replicators that are connected by

another superimposed autocatalytic cycle. Our study describes a mutualistic relationship between two replicators, each catalysing the formation of the other, that are linked by a superimposed catalytic cycle. Although the kinetic data suggest the intermediary of higher-order species in the autocatalytic processes, the present system should not be referred to as an example of a minimal hypercycle in the absence of direct experimental evidence for the autocatalytic cross-coupling between replicators. □

# The complete genome sequence of the hyperthermophilic, sulphate-reducing archaeon *Archaeoglobus fulgidus*

Hans-Peter Klenk, Rebecca A. Clayton, Jean-Francois Tomb, Owen White, Karen E. Nelson, Karen A. Ketchum, Robert J. Dodson, Michelle Gwinn, Erin K. Hickey, Jeremy D. Peterson, Delwood L. Richardson, Anthony R. Kerlavage, David E. Graham, Nikos C. Kyrpides, Robert D. Fleischmann, John Quackenbush, Norman H. Lee, Granger G. Sutton, Steven Gill, Ewen F. Kirkness, Brian A. Dougherty, Keith McKenney, Mark D. Adams, Brendan Loftus, Scott Peterson, Claudia I. Reich, Leslie K. McNeil, Jonathan H. Badger, Anna Glodek, Lixin Zhou, Ross Overbeek, Jeannine D. Gocayne, Janice F. Weidman, Lisa McDonald, Teresa Utterback, Matthew D. Cotton, Tracy Spriggs, Patricia Artiach, Brian P. Kaine, Sean M. Sykes, Paul W. Sadow, Kurt P. D'Andrea, Cheryl Bowman, Claire Fujii, Stacey A. Garland, Tanya M. Mason, Gary J. Olsen, Claire M. Fraser, Hamilton O. Smith, Carl R. Woese & J. Craig Venter

*Nature* **390**, 364–370 (1997)

The pathway for sulphate reduction is incorrect as published: in Fig. 3 on page 367, adenylyl sulphate 3-phosphotransferase (*cysC*) is not needed in the pathway as outlined, as adenylyl sulphate reductase (*aprAB*) catalyses the first step in the reduction of adenylyl sulphate. The correct sequence of reactions is: sulphate is first activated to adenylyl sulphate, then reduced to sulphite and subsequently to sulphide. The enzymes catalysing these reactions are: sulphate adenylyltransferase (*sat*), adenylylsulphate reductase (*aprAB*), and sulphite reductase (*dsrABD*). We thank Jens-Dirk Schwenn for bringing this error to our attention. □

# The complete genome sequence of the hyperthermophilic, sulphate-reducing archaeon *Archaeoglobus fulgidus*

Hans-Peter Klenk\*, Rebecca A. Clayton\*, Jean-Francois Tomb\*, Owen White\*, Karen E. Nelson\*, Karen A. Ketchum\*, Robert J. Dodson\*, Michelle Gwinn\*, Erin K. Hickey\*, Jeremy D. Peterson\*, Delwood L. Richardson\*, Anthony R. Kerlavage\*, David E. Graham†, Nikos C. Kyrpides†, Robert D. Fleischmann\*, John Quackenbush\*, Norman H. Lee\*, Granger G. Sutton\*, Steven Gill\*, Ewen F. Kirkness\*, Brian A. Dougherty\*, Keith McKenney\*, Mark D. Adams\*, Brendan Loftus\*, Scott Peterson\*, Claudia I. Reich†, Leslie K. McNeil†, Jonathan H. Badger†, Anna Glodek\*, Lixin Zhou\*, Ross Overbeek‡, Jeannine D. Gocayne\*, Janice F. Weidman\*, Lisa McDonald\*, Teresa Utterback\*, Matthew D. Cotton\*, Tracy Spriggs\*, Patricia Artiach\*, Brian P. Kaine†, Sean M. Sykes\*, Paul W. Sadow\*, Kurt P. D'Andrea\*, Cheryl Bowman\*, Claire Fujii\*, Stacey A. Garland\*, Tanya M. Mason\*, Gary J. Olsen†, Claire M. Fraser\*, Hamilton O. Smith\*, Carl R. Woese† & J. Craig Venter\*

\* The Institute for Genomic Research (TIGR), Rockville, Maryland 20850, USA

† Department of Microbiology, University of Illinois, Champaign-Urbana, Illinois 61801, USA

‡ Mathematics and Computer Science Division, Argonne National Laboratory, Illinois 60439, USA

***Archaeoglobus fulgidus* is the first sulphur-metabolizing organism to have its genome sequence determined. Its genome of 2,178,400 base pairs contains 2,436 open reading frames (ORFs). The information processing systems and the biosynthetic pathways for essential components (nucleotides, amino acids and cofactors) have extensive correlation with their counterparts in the archaeon *Methanococcus jannaschii*. The genomes of these two Archaea indicate dramatic differences in the way these organisms sense their environment, perform regulatory and transport functions, and gain energy. In contrast to *M. jannaschii*, *A. fulgidus* has fewer restriction-modification systems, and none of its genes appears to contain inteins. A quarter (651 ORFs) of the *A. fulgidus* genome encodes functionally uncharacterized yet conserved proteins, two-thirds of which are shared with *M. jannaschii* (428 ORFs). Another quarter of the genome encodes new proteins indicating substantial archaeal gene diversity.**

Biological sulphate reduction is part of the global sulphur cycle, ubiquitous in the earth's anaerobic environments, and is essential to the basal workings of the biosphere. Growth by sulphate reduction is restricted to relatively few groups of prokaryotes; all but one of these are Eubacteria, the exception being the archaeal sulphate reducers in the Archaeoglobales<sup>1,2</sup>. These organisms are unique in that they are unrelated to other sulphate reducers, and because they grow at extremely high temperatures<sup>3</sup>. The known Archaeoglobales are strict anaerobes, most of which are hyperthermophilic marine sulphate reducers found in hydrothermal environments<sup>2,4</sup> and in subsurface oil fields<sup>5</sup>. High-temperature sulphate reduction by *Archaeoglobus* species contributes to deep subsurface oil-well 'souring' by producing iron sulphide, which causes corrosion of iron and steel in oil- and gas-processing systems<sup>5</sup>.

*Archaeoglobus fulgidus* VC-16 (refs 2, 4) is the type strain of the Archaeoglobales. Cells are irregular spheres with a glycoprotein envelope and monopolar flagella. Growth occurs between 60 and 95 °C, with optimum growth at 83 °C and a minimum division time of 4 h. The organism grows organoheterotrophically using a variety of carbon and energy sources, but can grow lithoautotrophically on hydrogen, thiosulphate and carbon dioxide<sup>6</sup>. We sequenced the genome of *A. fulgidus* strain VC-16 as an example of a sulphur-metabolizing organism and to gain further insight into the Archaea<sup>7,8</sup> through genomic comparison with *Methanococcus jannaschii*<sup>9</sup>.

## General features of the genome

The genome of *A. fulgidus* consists of a single, circular chromosome of 2,178,400 base pairs (bp) with an average of 48.5% G+C content

(Fig. 1). There are three regions with low G+C content (<39%), two rich in genes encoding enzymes for lipopolysaccharide (LPS) biosynthesis, and two regions of high G+C content (>53%), containing genes for large ribosomal RNAs, proteins involved in haem biosynthesis (*hemAB*), and several transporters (Table 1). Because the origins of replication in Archaea are not characterized, we arbitrarily designated base pair one within a presumed non-coding region upstream of one of three areas containing multiple short repeat elements.

**Open reading frames.** Two independent coding analysis programs and BLASTX<sup>10</sup> searches (see Methods) predicted 2,436 ORFs (Figs 1, 2, Tables 1, 2) covering 92.2% of the genome. The average size of the *A. fulgidus* ORFs is 822 bp, similar to that of *M. jannaschii* (856 bp), but smaller than that in the completely sequenced eubacterial genomes (949 bp). All ORFs were searched against a non-redundant protein database, resulting in 1,797 putative identifications that were assigned biological roles within a classification system adapted from ref. 11. Predicted start codons are 76% ATG, 22% GTG and 2% TTG. Unlike *M. jannaschii*, where 18 inteins were found in coding regions, no inteins were identified in *A. fulgidus*. Compared with *M. jannaschii*, *A. fulgidus* contains a large number of gene duplications, contributing to its larger genome size. The average protein relative molecular mass ( $M_r$ ) in *A. fulgidus* is 29,753, ranging from 1,939 to 266,571, similar to that observed in other prokaryotes. The isoelectric point (pI) of predicted proteins among sequenced prokaryotes exhibits a bimodal distribution with peaks at pIs of approximately 5.5 and 10.5. The exceptions to this are *Mycoplasma genitalium* in which the distribution is skewed towards high pI

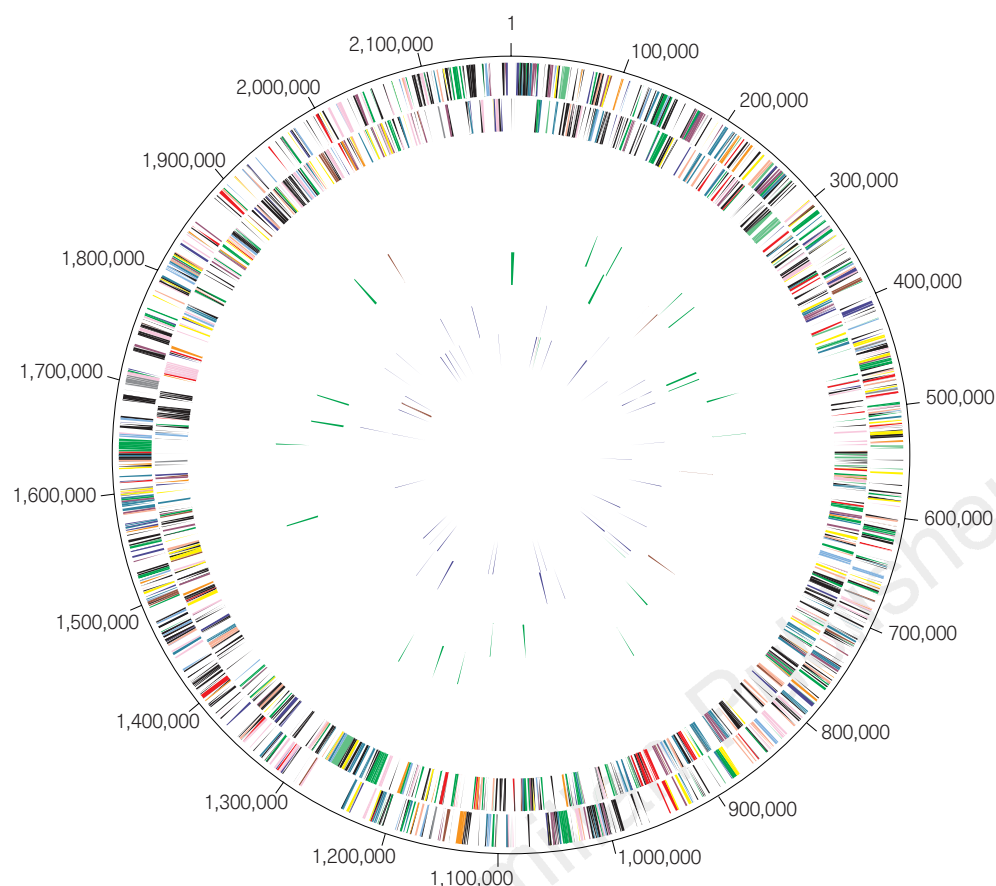


**Figure 1** Circular representation of the *A. fulgidus* genome. The outer circle shows predicted protein-coding regions on the plus strand classified by function according to the colour code in Fig. 2 (except for unknowns and hypotheticals, which are in black). Second circle shows predicted protein-coding regions on the minus strand. Third and fourth circles show IS elements (red) and other repeats (green) on the plus and minus strand. Fifth and sixth circles show tRNAs (blue), rRNAs (red) and sRNAs (green) on the plus and minus strand, respectively.

**Table 1 Genome features**

General		
Chromosome size:	2,178,400 bp	
Protein coding regions:	92.2%	
Stable RNAs:	0.4%	
<b>Predicted protein coding sequences:</b>		
Identified by database match:	2,436 (1.1 per kb)	
putative function assigned:	1,797	
homologues of <i>M. jannaschii</i> ORFs:	1,096	
conserved hypothetical proteins:	916	
No database match:	651	
Members of 242 paralogous families:	639	
Members of 158 families with known functions:	719	
	475	
<b>Stable RNAs</b>		
	Coordinates	
16S rRNA:	1,790,478–1,788,987	
23S rRNA:	1,788,751–1,785,820	
5S rRNA:	81,144–81,021	
7S RNA:	798,067–798,376	
RNase P:	86,281–86,032	
46 species of tRNA:	no significant clusters	
tRNAs with 15–62 bp introns:	Asp <sup>GUC</sup> , Glu <sup>UUC</sup> , Leu <sup>CAA</sup> , Trp <sup>CCA</sup> , Tyr <sup>GUA</sup>	
<b>Distinct G+C content regions</b>		
	Coordinates	
HGC-1, >53% G+C	1,786,000–1,797,000	
HGC-2, >53% G+C	2,158,000–2,159,000	
LGC-1, <39% G+C	281,000–284,000	
LGC-2, <39% G+C	544,000–550,000	
LGC-3, <39% G+C	1,175,000–1,177,000	
<b>Short, non-coding repeats</b>		
	Coordinates	
SR-1A, CTTTCAATCCCATTGTTGGTCTGATTTCAAC	147–4,213	
SR-1B, CTTTCAATCCCATTGTTGGTCTGATTTCAAC	398,368–401,590	
SR-2, CTTTCAATCTCCATTTTCAGGGCCTCCCTTTCTTA	1,690,930–1,694,104	
<b>Long, coding repeats</b>		
	Length	Copy number
LR-01 NADH-flavin oxidoreductase	1,886 bp	2 copies
LR-02 NifS, NifU + ORF	1,549 bp	2 copies
LR-03 ISA1214 putative transposase + ISORF2	1,214 bp	6 copies
LR-04 ISA1083 putative transposase + ISORF2	1,083 bp	3 copies
LR-05 type II secretion system protein	1,014 bp	4 copies
LR-06 ISA0963 putative transposase	963 bp	7 copies
LR-07 homologue of MJ0794	836 bp	3 copies
LR-08 conserved hypothetical protein	696 bp	2 copies
LR-09 conserved hypothetical protein	628 bp	2 copies

(median, 9.8) and *A. fulgidus* where the skew is toward low pI (median, 6.3).

**Multigene families.** In *A. fulgidus* 719 genes (30% of the total) belong to 242 families with two or more members (Table 1). Of these families, 157 contained genes with biological roles. Most of these families contain genes assigned to the 'energy metabolism', 'transport and binding proteins', and 'fatty acid and phospholipid metabolism' categories (Table 2). The superfamily of ATP-binding subunits of ABC transporters is the largest, containing 40 members. The importance of catabolic degradation and signal recognition systems is reflected by the presence of two large superfamilies: acyl-CoA ligases and signal-transducing histidine kinases. *A. fulgidus* does not contain a homologue of the large 16-member family found in *M. jannaschii*<sup>9</sup>.

**Repetitive elements.** Three regions of the *A. fulgidus* genome contain short (<40 bp) direct repeats (Table 1). Two regions (SR-1A and SR-1B) contain 48 and 60 copies, respectively, of an identical 30-bp repeat interspersed with unique sequences averaging 40 bp. The third region (SR-2) contains 42 copies of a 37-bp repeat similar in sequence to the SR-1 repeat and interspersed with unique sequence averaging 41 bp. These repeated sequences are similar to the short repeated sequences found in *M. jannaschii*.

Nine classes of long (>500 bp) repeated sequences with ≥95% sequence identity were found (LR1-LR9; Table 1). LR-3 is a novel element with 14-bp inverted repeats and two genes, one of which has weak similarity to a transposase from *Halobacterium salinarium*. One copy of LR-3 interrupts AF2090, a homologue of a large *M. jannaschii* gene encoding a protein of unknown function. LR-4 and LR-6 encode putative transposases not identified in *M. jannaschii* that may represent IS elements. The remaining LR elements are not similar to known IS elements.

### Central intermediary and energy metabolism

Sulphur oxide reduction may be the dominant respiratory process in anaerobic marine and freshwater environments, and is an important aspect of the sulphur cycle in anaerobic ecosystems<sup>12</sup>. In this pathway, sulphate (SO<sub>4</sub><sup>2-</sup>) is first activated to adenylylsulphate (adenosine-5'-phosphosulphate; APS), then reduced to sulphite and subsequently to sulphide<sup>11,13</sup> (Fig. 3). The most important enzyme in dissimilatory sulphate reduction, adenylylsulphate reductase, reduces the activated sulphate to sulphite, releasing AMP. In *A. fulgidus*, the APS reductase has a high degree of similarity and identical physiological properties to APS reductases in sulphate-reducing delta proteobacteria<sup>14</sup>. A desulphoviridin-type sulphite reductase then adds six electrons to sulphite to produce sulphide. As in the Eubacteria, three sulphite-reductase genes, *dsrABD*, constitute an operon. The genes for adenylylsulphate reductase and sulphate adenylyltransferase reside in a separate operon. In *A. fulgidus*, sulphate can be replaced as an electron acceptor by both thiosulphate (S<sub>2</sub>O<sub>3</sub><sup>2-</sup>) and sulphite (SO<sub>3</sub><sup>2-</sup>), but not by elemental sulphur.

*A. fulgidus* VC-16 has been shown to use lactate, pyruvate, methanol, ethanol, 1-propanol and formate as carbon and energy sources<sup>2</sup>. Glucose has been described as a carbon source<sup>1</sup>, but neither an uptake-transporter nor a catabolic pathway could be identified. Although it has been reported that *A. fulgidus* is incapable of growth on acetate<sup>6</sup>, multiple genes for acetyl-CoA synthetase (which converts acetate to acetyl-CoA) were found. The organism may degrade a variety of hydrocarbons and organic acids because of the presence of 57 β-oxidation enzymes, at least one lipase, and a minimum of five types of ferredoxin-dependent oxidoreductases (Fig. 3). The predicted β-oxidation system is similar to those in Eubacteria and mitochondria, and has not previously been described in the Archaea. *Escherichia coli* requires both the *fadD* and *fadL* gene products to import long-chain fatty acids across the cell envelope into the cytosol<sup>15</sup>. *A. fulgidus* has 14 acyl-CoA ligases related to *FadD*, but as expected given that it has no outer membrane, no

*FadL*. In *E. coli*, *FadB* has several metabolic functions, but in *A. fulgidus* these functions seem to be distributed among separate enzymes. For example, AF0435 encodes an orthologue of enoyl-CoA hydratase and resembles the amino-terminal domain of *FadB*. This gene is immediately upstream of a gene encoding an orthologue of 3-hydroxyacyl-CoA dehydrogenase that resembles the carboxy-terminal domain of *FadB*.

Acetyl-CoA is degraded by *A. fulgidus* through a C<sub>1</sub>-pathway, not by the citric acid cycle or glyoxylate bypass<sup>6,16,17</sup>. This degradation is catalysed through the carbon monoxide dehydrogenase (CODH) pathway that consists of a five-subunit acetyl-CoA decarboxylase/synthase complex (ACDS) and five enzymes that are typically involved in methanogenesis<sup>18</sup>. In *A. fulgidus*, however, reverse methanogenesis occurs, resulting in CO<sub>2</sub> production. All of the enzymes and cofactors of methanogenesis from formylmethanofuran to N<sup>5</sup>-methyltetrahydromethanopterin are used, but the absence of methyl-CoM reductase eliminates the possibility of methane production by conventional pathways. Production of trace amounts of methane (<0.1 μmol ml<sup>-1</sup>)<sup>19</sup> is probably a result of the reduction of N<sup>5</sup>-methyltetrahydromethanopterin to methane and tetrahydromethanopterin by carbon monoxide (CO) dehydrogenase.

*A. fulgidus* also contains genes suggesting it has a second CO dehydrogenase system, homologous to that which enables *Rhodospirillum rubrum* to grow without light using CO as its sole energy source. Genes were detected for the nickel-containing CO dehydrogenase (CooS), an iron-sulphur redox protein, and a protein associated with the incorporation of nickel in CooS. These represent elements of a system that could catalyse the conversion of CO and H<sub>2</sub>O to CO<sub>2</sub> and H<sub>2</sub>.

In contrast to *M. jannaschii*, *A. fulgidus* contains genes representing multiple catabolic pathways. Systems include CoA-SH-dependent ferredoxin oxidoreductases specific for pyruvate, 2-ketoisovalerate, 2-ketoglutarate and indolepyruvate, as well as a 2-oxoacid with little substrate specificity<sup>20,21</sup>. Four genes with similarity to the tungsten-containing aldehyde ferredoxin oxidoreductase were also found<sup>22</sup>.

Biochemical pathways characteristic of eubacterial metabolism, including the pentose-phosphate pathway, the Entner-Doudoroff pathway, glycolysis and gluconeogenesis, are either completely absent or only partly represented (Fig. 3). *A. fulgidus* does not have typical eubacterial polysaccharide biosynthesis machinery, yet it has been shown to produce a protein and carbohydrate-containing biofilm<sup>23</sup>. Nitrogen is obtained by importing inorganic molecules or degrading amino acids (Fig. 3); neither a glutamate dehydrogenase nor a relevant *fix* or *nif* gene is present.

The F<sub>420</sub>H<sub>2</sub>:quinone oxidoreductase complex<sup>24</sup> is recognized as

**Figure 2** Linear representation of the *A. fulgidus* genome illustrating the location of each predicted protein-coding region, RNA gene, and repeat element in the genome. Symbols for the transporters are as follows: AsO, arsenite; COH, sugar; P<sub>i</sub>, phosphate; aa2, dipeptide; NH<sub>4</sub><sup>+</sup>, ammonium; a/o, arginine/lysine/ornithine; s/p, spermidine/putrescine; glyc, glycerol; Cl<sup>-</sup>, chloride; Fe<sup>2+</sup>, iron(II); Fe<sup>3+</sup>, iron(III); I, L, V, branched-chain amino acids; P, proline; pan, pantothenate; rib, ribose; lac, lactate; Mg<sup>2+</sup>/Co<sup>2+</sup>, magnesium and cobalt; gln, glutamine; NO<sub>3</sub><sup>-</sup>, nitrate; ox/for, oxalate/formate; maln, malonic acid; Hg<sup>2+</sup>, mercury; phs, polysaccharide; SO<sub>4</sub><sup>2-</sup>, sulphate; OCN<sup>-</sup>, cyanate; hex, hexuronate; phs, polysialic acid; K<sup>+</sup>, potassium channel; H<sup>+</sup>/Na<sup>+</sup>, sodium/proton antiporter; Na<sup>+</sup>/Cl<sup>-</sup>, sodium- and chloride-dependent transporter; P/G, osmoprotection protein; Cu<sup>2+</sup>, copper-transporting ATPase; +?, cation-transporting ATPase; ?, ABC-transporter without known function. Triplets associated with tRNAs represent the anticodon sequence. Numbers associated with GES represent the number of membrane-spanning domains (MSDs) according to Goldman, Engelman and Steiz scale as determined by TopPred<sup>25</sup>. Genes whose identification is based on genes in *M. jannaschii* are indicated by circles. Of the 236 proteins containing at least one MSD, 124 of these had two or more MSDs.

the main generator of proton-motive force. However, our analysis indicates the presence of heterodisulphide reductase and several molybdopterin-binding oxidoreductases, with polysulphide, nitrate, dimethyl sulphoxide, and thiosulphate as potential substrates, which might contribute to energizing the cell membrane. *A. fulgidus*

contains a large number of flavoproteins, iron-sulphur proteins and iron-binding proteins that contribute to the general intracellular flow of electrons (Fig. 3). Detoxification enzymes include a peroxidase/catalase, an alkyl-hydroperoxide reductase, arsenate reductase, and eight NADH oxidases, presumably catalysing the

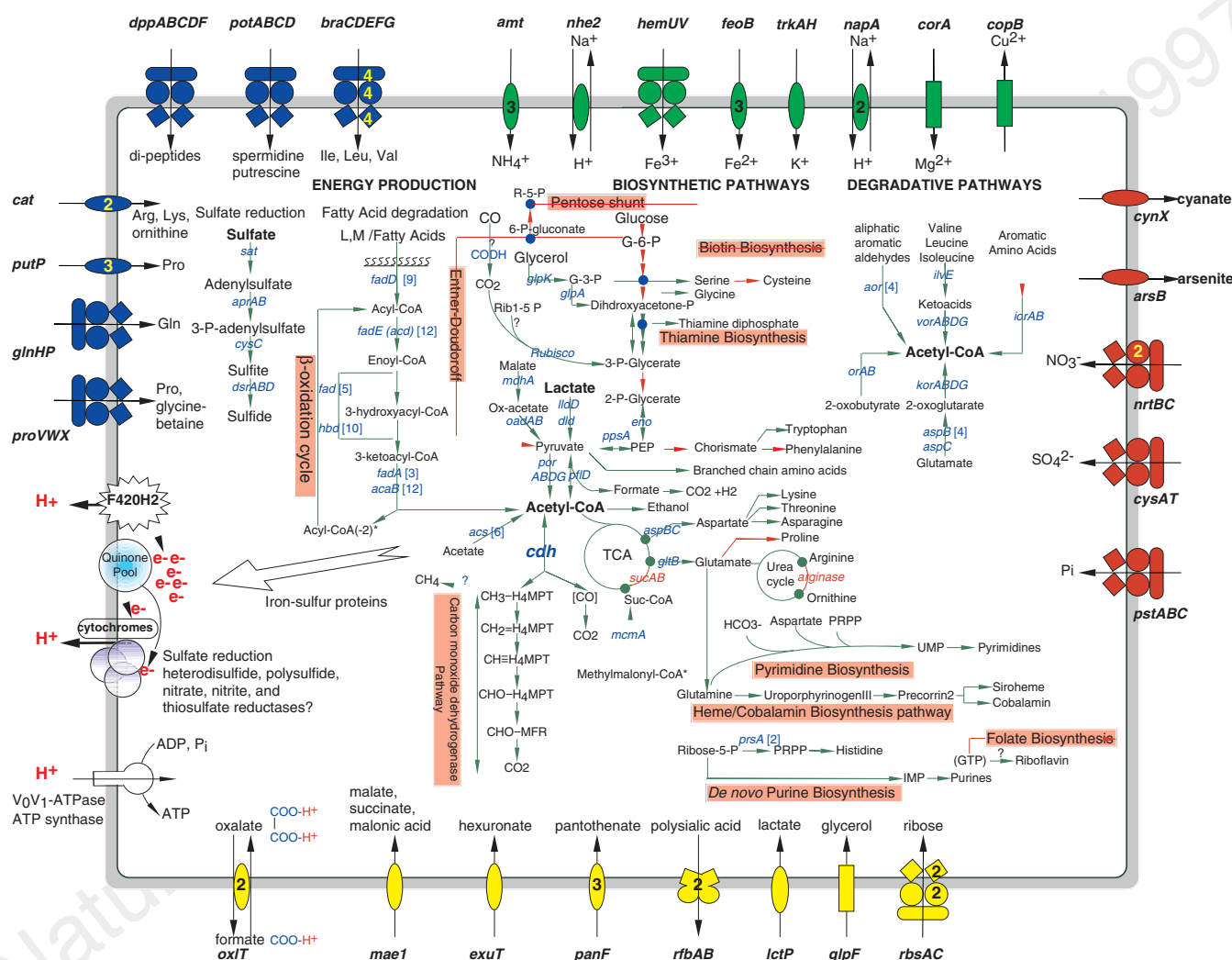


**Figure 3** An integrated view of metabolism and solute transport in *A. fulgidus*. Biochemical pathways for energy production, biosynthesis of organic compounds, and degradation of amino acids, aldehydes and acids are shown with the central components of *A. fulgidus* metabolism, sulphate, lactate and acetyl-CoA highlighted. Pathways or steps for which no enzymes were identified are represented by a red arrow. A question mark is attached to pathways that could not be completely elucidated. Macromolecular biosynthesis of RNA, DNA and ether lipids have been omitted. Membrane-associated reactions that establish the proton-motive force (PMF) and generate ATP (electron transport chain and  $V_0V_1$ -ATPase) are linked to cytosolic pathways for energy production. The oxalate-formate antiporters (*oxIT*) may also contribute to the PMF by mediating electrogenic anion exchange. Each gene product with a predicted function in ion or solute transport is illustrated. Proteins are grouped by substrate specificity with transporters for cations (green), anions (red), carbohydrates/organic alcohols/acids (yellow), and amino acids/peptides/amines (blue) depicted. Ion-coupled permeases are represented by ovals (*mae1*, *exuT*, *panF*, *lctP*, *arsB*, *cynX*, *napA*/*nhe2*, *amt*, *feoB*, *trkAH*, *cat* and *putP* encode transporters for malate, hexuronate, pantothenate, lactate, arsenite, cyanate, sodium, ammonium, iron (II), potassium, arginine/lysine and proline, respectively). ATP-binding cassette (ABC) transport systems are shown as composite figures of ovals, diamonds and circles (*proVWX*, *glnHPQ*, *dppABCD*, *potABCD*, *braCDEFG*, *hemUV*, *nrtBC*, *cysAT*, *pstABC*, *rbsAC*, *rbAB* correspond to gene products for proline, glutamine, dipeptide,

spermidine/putrescine, branch-chain amino acids, iron (III), nitrate, sulphate, phosphate, ribose and polysialic acid transport, respectively). All other porters drawn as rectangles (*glpF*, glycerol uptake facilitator; *copB*, copper transporting ATPase; *corA*, magnesium and cobalt transporter). Export and import of solutes is designated by arrows. The number of paralogous genes encoding each protein is indicated in brackets for cytoplasmic enzymes, or within the figure for transporters. Abbreviations: *acs*, acetyl-CoA synthetase; *aor*, aldehyde ferredoxin oxidoreductase; *aprAB*, adenylylsulphate reductase; *aspBC*, aspartate aminotransferase; *cdh*, acetyl-CoA decarboxylase/synthase complex; *cysC*, adenylylsulphate 3-phosphotransferase; *dld*, D-lactate dehydrogenase; *dsrABD*, sulphite reductase; *eno*, enolase; *fadA/acaB*, 3-ketoacyl-CoA thiolase; *fadD*, long-chain-fatty-acid-CoA ligase; *fad*, enoyl-CoA hydratase; *fadE (acd)*, acyl-CoA dehydrogenase; *glpA*, glycerol-3-phosphate dehydrogenase; *glpK*, glycerol kinase; *gltB*, glutamate synthase; *hbd*, 3-hydroxyacyl-CoA dehydrogenase; *ilvE*, branched-chain amino acid aminotransferase; *iorAB*, indolepyruvate ferredoxin oxidoreductase; *korABDG*, 2-ketoglutarate ferredoxin oxidoreductase; *lldD*, L-lactate dehydrogenase; *mcmA*, methylmalonyl-CoA mutase; *mdhA*, L-malate dehydrogenase; *oadAB*, oxaloacetate decarboxylase; *orAB*, 2-oxoacid ferredoxin oxidoreductase; *pfID*, pyruvate formate lyase 2; *porABDG*, pyruvate ferredoxin oxidoreductase; *ppsA*, phosphoenolpyruvate synthase; *prsA*, ribose-phosphate pyrophosphokinase; *sucAB*, 2-ketoglutarate dehydrogenase; *sat*, sulphate adenylyltransferase; TCA, tricarboxylic acid cycle; *vorABDG*, 2-ketoisovalerate ferredoxin oxidoreductase.

four-electron reduction of molecular oxygen to water, with the concurrent regeneration of NAD.

## Transporters

*A. fulgidus* may synthesize several transporters for the import of carbon-containing compounds, probably contributing to its ability to switch from autotrophic to heterotrophic growth<sup>5</sup>. Both *M. jannaschii* and *A. fulgidus* have branched-chain amino-acid ABC transport systems and a transporter for the uptake of arginine and lysine. *A. fulgidus* encodes proteins for dipeptide, spermidine/putrescine, proline/glycine-betaine and glutamine uptake, as well as transporters for sugars and acids, rather like the membrane systems described in eubacterial heterotrophs. These compounds provide the necessary substrates for numerous biosynthetic and degradative pathways (Fig. 3).

Many *A. fulgidus* redox proteins are predicted to require iron. Correspondingly, iron transporters have been identified for the import of both oxidized (Fe<sup>3+</sup>) and reduced (Fe<sup>2+</sup>) forms of iron. There are duplications in functional and regulatory genes in both systems. The uptake of Fe<sup>3+</sup> may depend on haemin or a haemin-like compound because *A. fulgidus* has orthologues to the eubacterial *hem* transport system proteins, HemU and HemV. *A. fulgidus* may also use the regulatory protein Fur to modulate Fe<sup>3+</sup> transport; this protein is not present in *M. jannaschii*. Fe<sup>2+</sup> uptake occurs through a modified Feo system containing FeoB. This is the third example of an isolated *feoB* gene: *M. jannaschii* and *Helicobacter pylori* also appear to lack *feoA*, implying that FeoA is not essential for iron transport in these organisms.

A complex suite of proteins regulates ionic homeostasis. Ten distinct transporters facilitate the flux of the physiological ions K<sup>+</sup>, Na<sup>+</sup>, NH<sub>4</sub><sup>+</sup>, Mg<sup>2+</sup>, Fe<sup>2+</sup>, Fe<sup>3+</sup>, NO<sub>3</sub><sup>-</sup>, SO<sub>4</sub><sup>2-</sup> and inorganic phosphate (P<sub>i</sub>). Most of these transporters have homologues in *M. jannaschii* and are therefore likely to be critical for nutrient acquisition during autotrophic growth. *A. fulgidus* has additional ion transporters for the elimination of toxic compounds including copper, cyanate and arsenite. As in *M. jannaschii*, the *A. fulgidus* genome contains two paralogous operons of cobalamin biosynthesis-cobalt transporters, *cbiMQO*.

## Sensory functions and regulation of gene expression

Consistent with its extensive energy-producing metabolism and versatile system for carbon utilization, *A. fulgidus* has complex sensory and regulatory networks. These networks contain over 55 proteins with presumed regulatory functions, including members of the ArsR, AsnC and Sir2 families, as well as several iron-dependent repressor proteins. There are at least 15 signal-transducing histidine kinases, but only nine response regulators; this difference suggests there is a high degree of cross-talk between kinases and regulators. Only four response regulators appear to be in operons with histidine kinases, including those in the methyl-directed chemotaxis system (Che), which lies adjacent to the flagellar biosynthesis operon. Although rich in regulatory proteins, *A. fulgidus* apparently lacks regulators for response to amino-acid and carbon starvation as well as to DNA damage. Finally, *A. fulgidus* contains a homologue of the mammalian mitochondrial benzodiazepine receptor, which functions as a sensor in signal-transduction pathways<sup>25</sup>. These receptors have been previously identified only in Proteobacteria and Cyanobacteria<sup>25</sup>.

## Replication, repair and cell division

*A. fulgidus* possesses two family B DNA polymerases, both related to the catalytic subunit of the eukaryal delta polymerase, as previously observed in the Sulfolobales<sup>26</sup>. It also has a homologue of the proofreading  $\epsilon$  subunit of *E. coli* Pol III, not previously observed in the Archaea. The DNA repair system is more extensive than that found in *M. jannaschii*, including a homologue of the eukaryal Rad25, a 3-methyladenine DNA glycosylase, and exodeoxynuclease

III. As well as reverse gyrase, topoisomerase I (ref. 9), and topoisomerase VI (ref. 27), the genes for the first archaeal DNA gyrase were identified.

*A. fulgidus* lacks a recognizable type II restriction-modification system, but contains one type I system. In contrast, two type II and three type I systems were identified in *M. jannaschii*. No homologue of the *M. jannaschii* thermonuclease was identified.

The cell-division machinery is similar to that of *M. jannaschii*, with orthologues of eubacterial *fts* and eukaryal *cdc* genes. However, several *cdc* genes found in *M. jannaschii*, including homologues of *cdc23*, *cdc27*, *cdc47* and *cdc54*, appear to be absent in *A. fulgidus*.

## Transcription and translation

*A. fulgidus* and *M. jannaschii* have transcriptional and translational systems distinct from their eubacterial and eukaryal counterparts. In both, the RNA polymerase contains the large universal subunits and five smaller subunits found in both Archaea and eukaryotes. Transcription initiation is a simplified version of the eukaryotic mechanism<sup>28,29</sup>. However, *A. fulgidus* alone has a homologue of eukaryotic TBP-interacting protein 49 not seen in *M. jannaschii*, but apparently present in *Sulfolobus solfataricus*.

Translation in *A. fulgidus* parallels *M. jannaschii* with a few exceptions. The organism has only one rRNA operon with an Ala-tRNA gene in the spacer and lacks a contiguous 5S rRNA gene. Genes for 46 tRNAs were identified, five of which contain introns in the anticodon region that are presumably removed by the intron excision enzyme EndA. The gene for selenocysteine tRNA (SelC) was not found, nor were the genes for SelA, SelB and SelD. With the exception of Asp-tRNA<sup>GTC</sup> and Val-tRNA<sup>CAC</sup>, tRNA genes are not linked in the *A. fulgidus* genome. The RNA component of the tRNA maturation enzyme RNase P is present. Both *A. fulgidus* and *M. jannaschii* appear to possess an enzyme that inserts the tRNA-modified nucleoside archaeosine, but only *A. fulgidus* has the related enzyme that inserts the modified base queuine.

Both *A. fulgidus* and *M. jannaschii* lack glutamine synthetase and asparagine synthetase; the relevant tRNAs are presumably aminoacylated with glutamic and aspartic acids, respectively. An enzymatic *in situ* transamidation then converts the amino acid to its amide form, as seen in other Archaea and in Gram-positive Eubacteria<sup>30</sup>. Indeed, genes for the three subunits of the Glu-tRNA amidotransferase (*gatABC*) have been identified in *A. fulgidus*. The Lys aminoacyl-tRNA synthetase in both organisms is a class I-type, not a class II-type<sup>31</sup>. *A. fulgidus* possesses a normal tRNA synthetase for both Cys and Ser, unlike *M. jannaschii* in which the former was not identifiable and the latter was unusual<sup>9</sup>.

*M. jannaschii* has a single gene belonging to the TCP-1 chaperonin family, whereas *A. fulgidus* has two that encode subunits  $\alpha$  and  $\beta$  of the thermosome. Phylogenetic analysis of the archaeal TCP-1 family indicates that these *A. fulgidus* genes arose by a recent species-specific gene duplication, as is the case for the two subunits of the *Thermoplasma acidophilum* thermosome<sup>32</sup> and the *Sulfolobus shibatae* rosettasome<sup>33</sup>. As in *M. jannaschii*, no *dnaK* gene was identified.

## Biosynthesis of essential components

Like most autotrophic microorganisms, *A. fulgidus* is able to synthesize many essential compounds, including amino acids, cofactors, carriers, purines and pyrimidines. Many of these biosynthetic pathways show a high degree of conservation between *A. fulgidus* and *M. jannaschii*. These two Archaea are similar in their biosynthetic pathways for siroheme, cobalamin, molybdopterin, riboflavin, thiamin and nicotinate, the role category with greatest conservation between these two organisms being amino-acid biosynthesis. Of 78 *A. fulgidus* genes assigned to amino-acid biosynthetic pathways, at least 73 (94%) have homologues in *M. jannaschii*. For both archaeal species, amino-acid biosynthetic pathways resemble those of *Bacillus subtilis* more closely than

those of *E. coli*. For example, in *A. fulgidus* and *M. jannaschii*, tryptophan biosynthesis is accomplished by seven enzymes, TrpA, B, C, D, E, F, G as in *B. subtilis*, rather than by five enzymes, TrpA, B, C, D, E (including the bifunctional TrpC and TrpD) as found in *E. coli*.

No biotin biosynthetic genes were identified, yet biotin can be detected in *A. fulgidus* cell extracts<sup>34</sup>, and several genes encode a biotin-binding consensus sequence. Similarly, *A. fulgidus* lacks the genes for pyridoxine biosynthesis although pyridoxine can be found in cell extracts (albeit at lower levels than seen in *E. coli* and several Archaea<sup>34</sup>). No gene encoding ferrochelatase, the terminal enzyme in haem biosynthesis, has been identified, although *A. fulgidus* is known to use cytochromes<sup>34</sup>. These cofactors may be obtained by mechanisms that we have not recognized. Although all of the enzymes required for pyrimidine biosynthesis appear to be present, three enzymes in the purine pathway (GAR transformylase, AICAR formyltransferase and the ATPase subunit of AIR carboxylase) have not been identified, presumably because they exist as new isoforms.

The Archaea share a unique cell membrane composed of ether lipids containing a glycerophosphate backbone with a 2,3-*sn* stereochemistry<sup>35</sup> for which there are multiple biosynthetic pathways<sup>36</sup>. In the case of *Halobacterium cutirubrum*, the backbone is apparently obtained by enantiomeric inversion of *sn*-glycerol-3-phosphate; in *Sulfolobus acidocaldarius* and *Methanobacterium thermoautotrophicum*, *sn*-glycerol-1-phosphate dehydrogenase builds the backbone from dihydroxyacetonephosphate. An orthologue of *sn*-glycerol-1-phosphate dehydrogenase has been identified in *A. fulgidus*, suggesting that the latter pathway is present.

## Conclusions

Although *A. fulgidus* has been studied since its discovery ten years ago<sup>1</sup>, the completed genome sequence provides a wealth of new information about how this unusual organism exploits its environment. For example, its ability to reduce sulphur oxides has been well characterized, but genome sequence data demonstrate that *A. fulgidus* has a great diversity of electron transport systems, some of unknown specificity. Similarly, *A. fulgidus* has been characterized as a scavenger with numerous potential carbon sources, and its gene complement reveals the extent of this capability. *A. fulgidus* appears to obtain carbon from fatty acids through  $\beta$ -oxidation, from degradation of amino acids, aldehydes and organic acids, and perhaps from CO.

*A. fulgidus* has extensive gene duplication in comparison with other fully sequenced prokaryotes. For example, in the fatty acid and phospholipid metabolism category, there are 10 copies of 3-hydroxyacyl-CoA dehydrogenase, 12 copies of 3-ketoacyl-CoA thiolase, and 12 of acyl-CoA dehydrogenase. The duplicated proteins are not identical, and their presence suggests considerable metabolic differentiation, particularly with respect to the pathways for decomposing and recycling carbon by scavenging fatty acids. Other categories show similar, albeit less dramatic, gene redundancy. For example, there are six copies of acetyl-CoA synthetase and four aldehyde ferredoxin oxidoreductases for fermentation, as well as four copies of aspartate aminotransferase for amino-acid biosynthesis. These observations, together with the large number of paralogous gene families, suggest that gene duplication has been an important evolutionary mechanism for increasing physiological diversity in the Archaeoglobales.

A comparison of two archaeal genomes is inadequate to assess the diversity of the entire domain. Given this caveat, it is nevertheless possible to draw some preliminary conclusions from the comparison of *M. jannaschii* and *A. fulgidus*. A comparison of the gene content of these Archaea reveals that gene conservation varies significantly between role categories, with genes involved in transcription, translation and replication highly conserved; approximately 80% of the *A. fulgidus* genes in these categories have homologues in *M. jannaschii*. Biosynthetic pathways are also

highly conserved, with approximately 80% of the *A. fulgidus* biosynthetic genes having homologues in *M. jannaschii*. In contrast, only 35% of the *A. fulgidus* central intermediary metabolism genes have homologues, reflecting their minimal metabolic overlap.

Over half of the *A. fulgidus* ORFs (1,290) have no assigned biological role. Of these, 639 have no database match. The remaining 651, designated 'conserved hypothetical proteins', have sequence similarity to hypothetical proteins in other organisms, two-thirds with apparent homologues in *M. jannaschii*. These shared hypothetical proteins will probably add to our understanding of the genetic repertoire of the Archaea. Analysis of the *A. fulgidus* and other archaeal and eubacterial genomes will provide the information necessary to begin to define a core set of archaeal genes, as well as to better understand prokaryotic diversity. □

## Methods

**Whole-genome random sequencing procedure.** The type strain, *A. fulgidus* VC-16, was grown from a culture derived from a single cell isolated by optical tweezers<sup>37</sup> and provided by K. O. Stetter (University of Regensburg). Cloning, sequencing and assembly were essentially as described previously for genomes sequenced by TIGR<sup>38–40</sup>. One small-insert and one medium-insert plasmid library were generated by random mechanical shearing of genomic DNA. One large-insert lambda ( $\lambda$ ) library was generated by partial *Tsp509I* digestion and ligation to  $\lambda$ -DASHII/*EcoRI* vector (Stratagene). In the initial random sequencing phase, 6.7-fold sequence coverage was achieved with 27,150 sequences from plasmid clones (average read length 500 bases) and 1,850 sequences from  $\lambda$ -clones. Both plasmid and  $\lambda$ -sequences were jointly assembled using TIGR assembler<sup>41</sup>, resulting in 152 contigs separated by sequence gaps and five groups of contigs separated by physical gaps. Sequences from both ends of 560  $\lambda$ -clones served as a genome scaffold, verifying the orientation, order and integrity and the contigs. Sequence gaps were closed by editing the ends of sequence traces and/or primer walking on plasmid or  $\lambda$ -clones clones spanning the respective gap. Physical gaps were closed by combinatorial polymerase chain reaction (PCR) followed by sequencing of the PCR product. At the end of gap closure, 90 regions representing 0.33% of the genome had only single-sequence coverage. These regions were confirmed with terminator reactions to ensure a minimum of 2-fold sequence coverage for the whole genome. The final genome sequence is based on 29,642 sequences, with a 6.8-fold sequence coverage. The linkage between the terminal sequences of 2,101 clones from the small-insert plasmid library (average size 1,419 bp) and 8,726 clones from the medium-insert plasmid library (average size 2,954 bp) supported the genome scaffold formed by the  $\lambda$ -clones (average size 16,381 bp), with 96.9% of the genome covered by  $\lambda$ -clones. The reported sequence differs in 20 positions from the 14,389 bp of DNA in a total of 11 previously published *A. fulgidus* genes.

**ORF prediction and gene family identification.** Coding regions (ORFs) were identified using a combination strategy based on two programs. Initial sets of ORFs were derived with GeneSmith (H.O.S., unpublished), a program that evaluates ORF length, separation and overlap between ORFs, and with CRITICA (J.H.B. & G.J.O., unpublished), a coding region identification tool using comparative analysis. The two largely overlapping sets of ORFs were merged into one joint set containing all members of both initial sets. ORFs were searched against a non-redundant protein database using BLASTX<sup>10</sup> and those shorter than 30 codons 'coding' for proteins without a database match were eliminated. Frameshifts were detected and corrected where appropriate as described previously<sup>40</sup>. Remaining frameshifts are considered authentic and corresponding regions were annotated as 'authentic frameshift'. In total, 527 hidden Markov models, based upon conserved protein families (PFAM version 2.0), were searched with HMMER to determine ORF membership in families and superfamilies<sup>42</sup>. Families of paralogous genes were constructed as described previously<sup>40</sup>. TopPred<sup>43</sup> was used to identify membrane-spanning domains in proteins.

Received 9 September; accepted 4 November 1997.

1. Stetter, K. O., Lauerer, G., Thomm, M. & Neuner, A. Isolation of extremely thermophilic sulfate reducers: Evidence for a novel branch of archaeobacteria. *Science* **236**, 822–824 (1987).
2. Stetter, K. O., in *The Prokaryotes* (eds Balows, A., Trüper, H. G., Dworkin, M., Harder, W. & Schleifer, K. H.) 707–711 (Springer, Berlin, 1992).
3. Stetter, K. O. Microbial life in hyperthermal environments: Microorganisms from exotic environments continue to provide surprises about life's extremities. *ASM News* **61**, 285–290 (1995).

4. Stetter, K. O. *Archaeoglobus fulgidus* gen. nov., sp. nov.: a new taxon of extremely thermophilic archaeobacteria. *Syst. Appl. Microbiol.* **10**, 172–173 (1988).
5. Stetter, K. O. *et al.* Hyperthermophilic archaea are thriving in deep North Sea and Alaskan oil reservoirs. *Nature* **365**, 743–745 (1993).
6. Vorholt, J., Kunow, J., Stetter, K. O. & Thauer, R. K. Enzymes and coenzymes of the carbon monoxide dehydrogenase pathway for autotrophic CO<sub>2</sub> fixation in *Archaeoglobus lithotrophicus* and the lack of carbon monoxide dehydrogenase in the heterotrophic *A. profundus*. *Arch. Microbiol.* **163**, 112–118 (1995).
7. Woese, C. R. & Fox, G. E. Phylogenetic structure of the prokaryotic domain: The primary kingdoms. *Proc. Natl Acad. Sci. USA* **74**, 5088–5090 (1977).
8. Woese, C. R., Kandler, O. & Wheelis, M. L. Towards a natural system of organisms: proposal for the domains Archaea, Bacteria, and Eucarya. *Proc. Natl Acad. Sci. USA* **87**, 4576–4579 (1990).
9. Bult, C. J. *et al.* Complete genome sequence of the methanogenic archaeon *Methanococcus jannaschii*. *Science* **273**, 1058–1073 (1996).
10. Altschul, S. F., Gish, W., Miller, W., Myers, E. W. & Lipman, D. J. Basic local alignment search tool. *J. Mol. Biol.* **215**, 403–410 (1990).
11. Riley, M. Functions of gene products of *Escherichia coli*. *Microbiol. Rev.* **57**, 862–952 (1993).
12. Cooling, F. B. III, Maloney, C. L., Nagel, E., Tabinowski, J. & Odom, J. M. Inhibition of sulfate respiration by 1,8-dihydroxyanthraquinone and other anthraquinone derivatives. *Appl. Environ. Microbiol.* **62**, 2999–3004 (1996).
13. Thauer, R. K. & Kunow, J. in *Sulfate Reducing Bacteria* (ed. Barton, L. L.) 33–48 (Plenum, New York, 1995).
14. Speich, D. *et al.* Adenylylsulfate reductase from the sulfate-reducing archaeon *Archaeoglobus fulgidus*: cloning and characterization of the genes and comparison of the enzyme with other iron-sulfur flavoproteins. *Microbiology* **140**, 1273–1284 (1994).
15. Clark, D. P. & Cronan, J. E. Jr in *Escherichia coli and Salmonella typhimurium: Cellular and Molecular biology* (ed Neidhardt, F. C.) 343–357 (ASM Press, Washington DC, 1996).
16. Möller-zirkhan, D. & Thauer, R. K. Anaerobic lactate oxidation to 3 CO<sub>2</sub> by *Archaeoglobus fulgidus* via the carbon monoxide dehydrogenase pathway: demonstration of the acetyl-CoA carbon-carbon cleavage reaction in cell extracts. *Arch. Microbiol.* **153**, 215–218 (1990).
17. Schauder, R., Eikmanns, B., Thauer, R. K., Widdel, F. & Fuchs, G. Acetate oxidation to CO<sub>2</sub> in anaerobic-bacteria via a novel pathway not involving reactions of the citric-acid cycle. *Arch. Microbiol.* **145**, 162–172 (1986).
18. Dai, Y.-R. *et al.* Acetyl-CoA decarbonylase/synthase complex from *Archaeoglobus fulgidus*: purification, characterization, and properties. *Arch. Microbiol.* (submitted).
19. Gorris, L. G. M., Voet, A. C. W. A. & van der Drift, C. Structural characteristics of methanogenic cofactors in the non-methanogenic archaeobacterium *Archaeoglobus fulgidus*. *BioFactors* **3**, 29–35 (1991).
20. Zhang, Q., Iwasaki, T., Wakagi, T. & Oshima, T. 2-oxoacid:ferredoxin oxidoreductase from the thermoacidophilic archaeon, *Sulfolobus* sp. strain 7. *J. Biochem.* **120**, 587–599 (1996).
21. Tersteegen, A., Linder, D., Thauer, R. K. & Hedderich, R. Structures and functions of four anabolic 2-oxoacid oxidoreductases in *Methanobacterium thermoautotrophicum*. *Eur. J. Biochem.* **244**, 862–868 (1997).
22. Kletzin, A. & Adams, M. W. W. Molecular and phylogenetic characterization of pyruvate and 2-ketoisovalerate ferredoxin oxidoreductases from *Pyrococcus furiosus* and pyruvate ferredoxin oxidoreductase from *Thermotoga maritima*. *J. Bacteriol.* **178**, 248–257 (1996).
23. LaPaglia, C. & Hartzell, P. L. Stress-induced production of biofilm in the hyperthermophile *Archaeoglobus fulgidus*. *Appl. Environ. Microbiol.* **63**, 3158–3163 (1997).
24. Kunow, J., Linder, D., Stetter, K. O. & Thauer, R. K. F<sub>120</sub>H<sub>2</sub>: quinone oxidoreductase from *Archaeoglobus fulgidus*—characterization of a membrane-bound multilubunit complex containing FAD and iron–sulfur clusters. *Eur. J. Biochem.* **223**, 503–511 (1994).
25. Yeliseev, A. A., Krueger, K. E. & Kaplan, S. A mammalian mitochondrial drug receptor functions as a bacterial “oxygen” sensor. *Proc. Natl Acad. Sci. USA* **94**, 5101–5106 (1997).
26. Edgell, D. R., Klenk, H.-P. & Doolittle, W. F. Gene duplications in evolution of archaeal family B DNA polymerases. *J. Bacteriol.* **179**, 2632–2640 (1997).
27. Bergerat, A. *et al.* An atypical topoisomerase II from archaea with implications for meiotic recombination. *Nature* **386**, 414–417 (1997).
28. Marsh, T. L., Reich, C. I., Whitelock, R. B. & Olsen, G. J. Transcription factor IID in the Archaea: sequences in the *Thermococcus celer* genome would encode a product closely related to the TATA-binding protein of eukaryotes. *Proc. Natl Acad. Sci. USA* **91**, 4180–4184 (1994).
29. Kosa, P. E., Ghosh, G., DeDecker, B. S. & Sigler, P. B. The 2.1-Å crystal structure of an archaeal preinitiation complex: TATA-box-binding protein/transcription factor (II)B core/TATA-box. *Proc. Natl Acad. Sci. USA* **94**, 6042–6047 (1997).
30. Curnow, A. W. *et al.* Glu-tRNA<sup>Gln</sup> amidotransferase: a novel heterotrimeric enzyme required for correct decoding of glutamine codons during translation. *Proc. Natl Acad. Sci. USA* **94**, 11819–11826 (1997).
31. Ibba, M., Bobo, J. L., Rosa, P. A. & Soll, D. Archaeal-type lysyl-tRNA synthetase in the Lyme disease spirochete *Borrelia burgdorferi*. *Proc. Natl Acad. Sci. USA* (submitted).
32. Waldmann, T., Lupas, A., Kellermann, J., Peters, J. & Baumeister, W. Primary structure of the thermosome from *Thermoplasma acidophilum*. *Hoppe-Seyler's Biol. Chem.* **376**, 119–126 (1995).
33. Kagawa, H. K. *et al.* The 60 kDa heat shock proteins in the hyperthermophilic archaeon *Sulfolobus shibatae*. *J. Mol. Biol.* **253**, 712–725 (1995).
34. Noll, K. M. & Barber, T. S. Vitamin contents of archaeobacteria. *J. Bacteriol.* **170**, 4315–4321 (1988).
35. Thornebene, T. G. & Langworthy, T. A. Diphytanyl and dibiphytanyl glycerol ether lipids of methanogenic archaeobacteria. *Science* **203**, 51–53 (1979).
36. Nishihara, M. & Koga, Y. sn-glycerol-1-phosphate dehydrogenase in *Methanobacterium thermoautotrophicum*: key enzyme in biosynthesis of the enantiomeric glycerophosphate backbone of other phospholipids of archaeobacteria. *J. Biochem.* **117**, 933–935 (1995).
37. Huber, R. *et al.* Isolation of a hyperthermophilic archaeum predicted by *in situ* RNA analysis. *Nature* **376**, 57–58 (1995).
38. Fleischmann, R. D. *et al.* Whole-genome random sequencing and assembly of *Haemophilus influenzae* Rd. *Science* **269**, 496–511 (1995).
39. Fraser, C. M. *et al.* The minimal gene complement of *Mycoplasma genitalium*. *Science* **270**, 397–403 (1995).
40. Tomb, J.-F. *et al.* The complete genome sequence of the gastric pathogen *Helicobacter pylori*. *Nature* **388**, 539–547 (1997).
41. Sutton, G. G., White, O., Adams, M. D. & Kerlavage, A. R. TIGR Assembler: A new tool for assembling large shotgun sequencing projects. *Genome Sequence Technol.* **1**, 9–19 (1995).
42. Sonnhammer, E. L., Eddy, S. R. & Durbin, R. Pfam: A comprehensive database of protein families based on seed alignments. *Proteins* **28**, 405–420 (1997).
43. Claros, M. G. & von Heijne, G. TopPred II: an improved software for membrane protein structure predictions. *Comput. Appl. Biosci.* **10**, 685–686 (1994).

**Acknowledgements.** We thank M. Heaney, J. Scott and R. Shirley for software and database support; V. Sapiro, B. Vincent, J. Meehan and D. Maas for computer system support; B. Cameron and D. J. Doyle for editorial assistance; and K. O. Stetter for providing *A. fulgidus* VC-16. This work was supported by the US Department of Energy.

Correspondence and requests for materials should be addressed to J.C.V. (e-mail: gaf@tigr.org). The annotated genome sequence and the gene family alignments are available on the World-Wide Web at <http://www.tigr.org/tdb/mdb/afdb/afdb.html>. The sequence has been deposited in GenBank with accession number AE000782.





**Table 2. List of *A. fulgidus* genes with putative identification. Gene numbers correspond to those in Fig. 2. Percentages represent per cent identities.**

AMINO ACID BIOSYNTHESIS		CELLULAR PROCESSES	
<i>General</i>		<i>General</i>	
AF0906	hydantoin utilization protein A (hyaA) 27.4%	AF1040	chemotaxis histidine kinase (cheA) 41.9%
<i>Aromatic amino acid family</i>		AF1035	chemotaxis histidine kinase, putative 25.3%
AF0228	3-dehydroquinate dehydratase (aroD) 36.8%	AF1036	chemotaxis histidine kinase, putative 30.4%
AF1497	5-enolpyruvylshikimate 3-phosphate synthase (aroA) 41.5%	AF1037	chemotaxis protein methyltransferase (cheF) 33.2%
AF1603	anthranilate synthase component I (trpE) 43.7%	AF1042	chemotaxis response regulator (cheY) 62.9%
AF1604	anthranilate synthase component II (trpD) 43.8%	AF1034	methyl-accepting chemotaxis protein (IttC-1) 27.5%
AF1602	anthranilate synthase component II (trpG) 50.0%	AF1045	methyl-accepting chemotaxis protein (IttC-2) 29.6%
AF0227	chorismate mutase/prephenate dehydratase (pheA) 32.2%	AF1041	protein-glutamate methyltransferase (cheB) 43.3%
AF0870	chorismate synthase (aroC) 55.3%	AF1032	purine NTPase, putative 32.2%
AF1601	phosphoribosyl anthranilate isomerase (trpF) 37.1%	AF1044	purine-binding chemotaxis protein (cheW) 40.4%
AF2327	shikimate 5-dehydrogenase (aroE) 43.1%	<i>Cell division</i>	
AF0343	tryptophan repressor binding protein (wrbA) 46.6%	AF0517	cell division control protein 21 (cdc21) 32.8%
AF1599	tryptophan synthase, subunit alpha (trpA) 39.5%	AF1297	cell division control protein 48, AAA family (cdc48-1) 69.1%
AF1240	tryptophan synthase, subunit beta (trpB-1) 39.4%	AF2098	cell division control protein 48, AAA family (cdc48-2) 62.0%
AF1600	tryptophan synthase, subunit beta (trpB-2) 64.1%	AF0244	cell division control protein 6, putative 27.5%
<i>Aspartate family</i>		AF1285	cell division control protein, AAA family, putative 49.3%
AF2112	5-methyltetrahydropteroyltryglutamate-homocysteine methyltransferase (metE) 28.1%	AF0696	cell division inhibitor (minD-1) 55.0%
AF0882	asparaginase (asnA) 45.9%	AF1937	cell division inhibitor (minD-2) 32.8%
AF1439	asparagine synthetase (asnB) 36.9%	AF2051	cell division protein (ftsI) 40.8%
AF2366	aspartate aminotransferase (aspB-1) 42.3%	AF0570	cell division protein (ftsZ-2) 61.4%
AF2129	aspartate aminotransferase (aspB-2) 45.4%	AF0837	cell division protein pelta (pelA) 41.7%
AF1623	aspartate aminotransferase (aspB-3) 39.4%	AF1215	cell division protein, putative 32.8%
AF0409	aspartate aminotransferase (aspB-4) 45.2%	AF0238	centromere/microtubule-binding protein (cbf5) 58.8%
AF1417	aspartate aminotransferase (aspC) 46.2%	AF1558	chromosome segregation protein (smc1) 32.8%
AF0700	aspartate kinase (lysC) 49.1%	AF1822	serine/threonine phosphatase (ppa) 31.9%
AF1422	aspartate racemase 48.0%	<i>Chaperones</i>	
AF1506	aspartate-semialdehyde dehydrogenase (asd) 60.9%	AF1296	small heat shock protein (hsp20-1) 52.3%
AF0800	diaminopimelate decarboxylase (lysA) 45.6%	AF1971	small heat shock protein (hsp20-2) 38.1%
AF0747	diaminopimelate epimerase (dapF) 45.8%	AF2238	thermosome, subunit alpha (thsA) 70.6%
AF0909	dihydrodipicolinate reductase (dapB) 48.6%	AF1451	thermosome, subunit beta (thsB) 68.2%
AF0910	dihydrodipicolinate synthase (dapA) 51.0%	<i>Chromosome-associated protein</i>	
AF0935	homoserine dehydrogenase (hom) 47.9%	AF0337	archaeal histone A1 (hpyA1-1) 64.6%
AF0886	S-adenosylhomocysteine hydrolase (ahcY-1) 31.7%	AF1493	archaeal histone A1 (hpyA1-2) 69.7%
AF2000	S-adenosylhomocysteine hydrolase (ahcY-2) 67.3%	<i>Detoxification</i>	
AF0051	succinyl-diaminopimelate desuccinylase (dapE-1) 30.5%	AF2173	2-nitropropane dioxygenase (ncd2) 39.7%
AF0904	succinyl-diaminopimelate desuccinylase (dapE-2) 43.8%	AF0370	alkyl hydroperoxide reductase 73.5%
AF0551	threonine synthase (thrC-1) 40.5%	AF1361	arsenate reductase (arsC) 30.5%
AF1316	threonine synthase (thrC-2) 61.0%	AF0550	N-ethylmalmine chloroxydrolase (trzA-1) 45.9%
<i>Glutamate family</i>		AF0997	N-ethylmalmine chloroxydrolase (trzA-2) 44.5%
AF1280	acetylglutamate kinase (argB) 56.1%	AF0254	NADH oxidase (noxA-1) 35.1%
AF2286	acetylglutamate kinase, putative 23.0%	AF0395	NADH oxidase (noxA-2) 35.5%
AF0080	acetylglutamate aminotransferase (argD-1) 48.3%	AF0400	NADH oxidase (noxA-3) 40.8%
AF1815	acetylornithine aminotransferase (argD-2) 36.2%	AF0951	NADH oxidase (noxA-4) 36.7%
AF0522	acetylornithine deacetylase (argE) 29.4%	AF1858	NADH oxidase (noxA-5) 34.0%
AF0883	argininosuccinate lyase (argH) 42.2%	AF0485	NADH oxidase (noxB-1) 43.3%
AF2252	argininosuccinate synthetase (argG) 62.0%	AF1282	NADH oxidase (noxB-2) 42.9%
AF1147	glutamate N-acetyltransferase (argJ) 47.8%	AF0226	NADH oxidase (noxC) 38.4%
AF0953	glutamate synthase (gltB) 57.9%	AF0515	NADH oxidase, putative 25.5%
AF0949	glutamine synthetase (glnA) 43.3%	AF2233	peroxidase / catalase (perA) 62.9%
AF2071	N-acetyl-gamma-glutamyl-phosphate reductase (argC) 53.3%	<i>Protein and peptide secretion</i>	
AF1255	ornithine carbamoyltransferase (argF) 51.7%	AF1283	protein translocase, subunit SEC61 alpha (secY) 50.0%
<i>Pyruvate family</i>		AF0636	protein translocase, subunit SEC61 gamma (secE) 25.0%
AF0957	2-isopropylmalate synthase (leuA-1) 53.5%	AF2062	signal recognition particle receptor (dps) 54.8%
AF0219	2-isopropylmalate synthase (leuA-2) 53.9%	AF1258	signal recognition particle, subunit SRP19 (srp19) 36.6%
AF2199	3-isopropylmalate dehydratase, large subunit (leuC) 49.3%	AF0622	signal recognition particle, subunit SRP54 (srp54) 51.2%
AF0629	3-isopropylmalate dehydratase, small subunit (leuD-1) 55.4%	AF1791	signal sequence peptidase (sec1) 36.3%
AF1781	3-isopropylmalate dehydratase, small subunit (leuD-2) 57.1%	AF1657	signal sequence peptidase (spe21) 47.0%
AF0628	3-isopropylmalate dehydrogenase (leuB) 59.2%	AF1655	signal sequence peptidase, putative 34.5%
AF1720	acetoacetylase synthase, large subunit (ilv-1) 57.5%	AF0338	type II secretion system protein (gspe-1) 38.5%
AF1780	acetoacetylase synthase, large subunit (ilv-2) 32.1%	AF0659	type II secretion system protein (gspe-2) 38.2%
AF2015	acetoacetylase synthase, large subunit (ilv-3) 34.1%	AF0996	type II secretion system protein (gspe-3) 41.7%
AF2100	acetoacetylase synthase, large subunit (ilv-4) 38.4%	AF1049	type II secretion system protein (gspe-4) 46.5%
AF1719	acetoacetylase synthase, small subunit (ilvN) 60.4%	<b>CENTRAL INTERMEDIARY METABOLISM</b>	
AF1672	acetoacetylase synthase, small subunit, putative 29.7%	<i>Degradation of polysaccharides</i>	
AF0933	branched-chain amino acid aminotransferase (ilvE) 59.0%	AF1207	2-deoxy-D-glucanase 3-dehydrogenase (kduD) 45.3%
AF1014	dihydroxy-acid dehydratase (ilvD) 54.5%	AF1795	endoglucanase (celM) 55.4%
AF1985	ketol-acid reductoisomerase (ilvC) 61.8%	<i>Phosphorus compounds</i>	
<i>Serine family</i>		AF0756	exopolysphatase (ppx1) 55.1%
AF0813	phosphoglycerate dehydrogenase (serA) 48.8%	<i>Polyamine biosynthesis</i>	
AF2138	phosphoserine phosphatase (serB) 50.7%	AF0646	agmatinase (speB) 33.3%
AF0273	sarcosine oxidase, subunit alpha (soxA) 31.1%	AF2334	spermidine synthase (speE) 37.1%
AF0274	sarcosine oxidase, subunit beta (soxB) 26.5%	<i>Polysaccharides - (cytoplasmic)</i>	
AF0852	serine hydroxymethyltransferase (glyA) 56.1%	AF0599	dolichol phosphate mannose synthase, putative 32.1%
<i>Histidine family</i>		<i>Sulfur metabolism</i>	
AF0690	ATP phosphoribosyltransferase (hisG) 31.9%	AF0288	adenylylsulfate 3-phosphotransferase (cysC) 52.0%
AF0212	histidinol dehydrogenase (hisD) 51.2%	AF1670	adenylylsulfate reductase, subunit A (aprA) 96.0%
AF2002	histidinol-phosphate aminotransferase (hisC-1) 39.8%	AF1669	adenylylsulfate reductase, subunit B (aprB) 97.3%
AF2024	histidinol-phosphate aminotransferase (hisC-2) 36.8%	AF1667	sulfate adenylyltransferase (sat) 28.4%
AF0985	imidazoleglycerol-phosphate dehydrogenase/histidinol-phosphatase (hisB) 42.2%	AF2228	sulfite reductase, desulfoavidin-type subunit gamma (dsvC) 41.3%
AF0819	imidazoleglycerol-phosphate synthase, cyclase subunit (hisF) 67.0%	AF0423	sulfite reductase, subunit alpha (dsrA) 100.0%
AF2285	imidazoleglycerol-phosphate synthase, subunit H (hisH) 44.4%	AF0424	sulfite reductase, subunit beta (dsrB) 100.0%
AF0509	imidazoleglycerol-phosphate synthase, subunit I, putative 43.2%	AF0425	sulfite reductase, subunit gamma (dsrD) 97.4%
AF1950	phosphoribosyl-AMP cyclohydrolase/phosphoribosyl-ATP pyrophosphorylase (hisE) 59.6%	<i>Other</i>	
AF0713	phosphoribosylformimino-5-aminoimidazole carboxamide ribotide isomerase (hisA-1) 37.5%	AF1706	2-hydroxy-6-oxo-6-phenylhexa-2,4-dienoic acid hydrolyase (pcbD) 29.4%
AF0986	phosphoribosylformimino-5-aminoimidazole carboxamide ribotide isomerase (hisA-2) 42.2%	AF0675	2-hydroxy-6-oxohepta-2,4-dienoate hydrolyase (todF) 26.3%
<b>BIOSYNTHESIS OF COFACTORS, PROSTHETIC GROUPS, AND CARRIERS</b>		AF0091	2-hydroxyhepta-2,4-diene-1,7-dioate isomerase (hpcE-1) 44.5%
<i>General</i>		AF2225	2-hydroxyhepta-2,4-diene-1,7-dioate isomerase (hpcE-2) 66.0%
AF1855	2,3-dihydroxybenzoate-AMP ligase (entE) 27.2%	AF0333	4-hydroxyphenylacetate 3-hydroxylase (hpaA-1) 22.4%
AF1070	coenzyme F390 synthetase (ftsA-1) 30.3%	AF0885	4-hydroxyphenylacetate 3-hydroxylase (hpaA-2) 26.0%
AF1671	coenzyme F390 synthetase (ftsA-2) 31.9%	AF1027	4-hydroxyphenylacetate 3-hydroxylase (hpaA-3) 21.0%
AF2013	coenzyme F390 synthetase (ftsA-3) 30.4%	AF0669	4-oxalocrotonate tautomerase, putative 31.9%
AF2151	isochorismatase (entB) 31.2%	AF0808	glycolate oxidase subunit (gldC) 32.0%
<i>Folic acid</i>		AF2216	methylmalonyl-CoA decarboxylase, biotin carboxyl carrier subunit (mrmC) 36.2%
AF1414	dihydropterolate synthase 40.8%	AF2217	methylmalonyl-CoA decarboxylase, subunit alpha (mrmA) 62.5%
<i>Heme and porphyrin</i>		AF1288	methylmalonyl-CoA mutase, subunit alpha (mutB), authentic frameshift 46.1%
AF1648	bacteriochlorophyll synthase, 33 kDa subunit 27.9%	AF2219	methylmalonyl-CoA mutase, subunit alpha, C-terminus (mcmA2) 48.7%
AF0464	bacteriochlorophyll synthase, 43 kDa subunit (chp-1) 23.7%	AF2215	methylmalonyl-CoA mutase, subunit alpha, N-terminus (mcmA1) 51.2%
AF1023	bacteriochlorophyll synthase, 43 kDa subunit (chp-2) 31.2%	AF2099	muconate cycloisomerase II (clicB) 24.9%
AF1637	bacteriochlorophyll synthase, 43 kDa subunit (chp-3) 27.0%	AF1425	phosphonopyruvate decarboxylase (bcpC-1) 35.0%
AF0037	cobalamin (5'-phosphate) synthase (cobS-1) 33.9%	AF1751	phosphonopyruvate decarboxylase (bcpC-2) 48.6%
AF2323	cobalamin (5'-phosphate) synthase (cobS-2) 34.4%	<b>ENERGY METABOLISM</b>	
AF0725	cobalamin biosynthesis precorrin-2 methylase (cbiG) 30.7%	<i>Amino acids and amines</i>	
AF0727	cobalamin biosynthesis precorrin-2 methyltransferase (cbiL) 31.5%	AF1958	2-hydroxyglutaryl-CoA dehydratase, subunit alpha (hgdA) 30.5%
AF0726	cobalamin biosynthesis precorrin-3 methylase (cbiF) 49.2%		
AF0724	cobalamin biosynthesis precorrin-3 methylase (cbiH) 49.0%		
AF0722	cobalamin biosynthesis precorrin-6Y methylase (cbiE) 32.4%		
AF0732	cobalamin biosynthesis precorrin-6W decarboxylase (cbiT) 30.8%		
AF1336	cobalamin biosynthesis protein (cbiB) 38.4%		
AF0723	cobalamin biosynthesis protein (cbiD) 36.3%		
AF0728	cobalamin biosynthesis protein (cbiM-1) 51.4%		
AF1843	cobalamin biosynthesis protein (cbiM-2) 41.2%		
AF0731	cobalt transport ATP-binding protein (cbiQ-1) 47.2%		
AF1841	cobalt transport ATP-binding protein (cbiQ-2) 41.1%		
AF0729	cobalt transport protein (cbiN) 56.0%		
AF0730	cobalt transport protein (cbiQ-1) 32.6%		
AF1842	cobalt transport protein (cbiQ-2) 30.3%		
AF1338	cobrynic acid synthase (cbiP) 44.5%		
AF2229	cobrynic acid, alpha-diamide synthase (cbiA) 42.3%		
AF1241	glutamate-1-semialdehyde aminotransferase (hemL) 54.3%		
AF1975	glutamyl-tRNA reductase (hemA) 42.7%		
AF1594	heme biosynthesis protein (nirH) 25.2%		
AF1125	heme biosynthesis protein (nir-1) 38.7%		
AF2009	heme biosynthesis protein (nir-2) 31.8%		
AF1593	heme d1 biosynthesis protein (nirD) 29.4%		
AF1311	oxygen-independent coproporphyrinogen III oxidase, putative 27.1%		
AF1242	porphobilinogen deaminase (hemC) 46.3%		
AF1974	porphobilinogen synthase (hemB) 60.4%		
AF1784	protoporphyrinogen oxidase (hemK) 33.5%		
AF0422	uroporphyrin-III-methyltransferase (cysG-1) 41.7%		
AF1243	uroporphyrin-III-methyltransferase (cysG-2) 52.5%		
AF0116	uroporphyrinogen III synthase (hemD) 27.4%		
<i>Menaquinone and ubiquinone</i>		AF2178	4-hydroxybenzoate octaprenyltransferase (ubiA) 41.6%
AF2404	4-hydroxybenzoate octaprenyltransferase, putative 30.6%	AF2413	coenzyme PQQ synthase protein (pqoE) 30.5%
AF1191	dihydroxynaphthoic acid synthase (menB) 54.6%	AF1561	octaprenyl-phosphate synthase (ispB) 33.2%
AF0140	ubiquinone/menaquinone biosynthesis methyltransferase (ubiE) 31.0%		
<i>Molybdopterin</i>		AF2006	molybdenum cofactor biosynthesis protein (moaA) 47.8%
AF0265	molybdenum cofactor biosynthesis protein (moaB) 44.4%	AF0265	molybdenum cofactor biosynthesis protein (moaB) 62.0%
AF2150	molybdenum cofactor biosynthesis protein (moaC) 50.8%	AF0931	molybdenum cofactor biosynthesis protein (moaA-1) 44.8%
AF0930	molybdenum cofactor biosynthesis protein (moaE-2) 40.3%	AF0161	molybdenum cofactor biosynthesis protein (moaA-3) 30.0%
AF1032	molybdenum cofactor biosynthesis protein (moaB) 49.3%	AF1624	molybdopterin converting factor, subunit 1 (moaD) 36.6%
AF2179	molybdopterin converting factor, subunit 2 (moaE) 33.3%	AF2005	molybdopterin-guanine dinucleotide biosynthesis protein A (mobA) 33.2%
AF2253	molybdopterin-guanine dinucleotide biosynthesis protein B (mobB) 40.0%		
<i>Pantothenate</i>		AF1645	pantothenate metabolism flavoprotein (dpp) 42.4%
AF0494	GTP cyclohydrolase II (ribA-1) 44.5%		
AF2107	GTP cyclohydrolase II (ribA-2) 47.1%		
AF1416	riboflavin synthase (ribC) 53.3%		
AF2128	riboflavin synthase, subunit beta (ribE) 75.9%		
AF2007	riboflavin-specific deaminase (ribD) 43.7%		
<i>Thiamine</i>		AF2075	hydroxyethylthiazole kinase (thiM) 33.6%
AF2208	hydroxymethylpyrimidine phosphate kinase (thiD) 35.5%	AF1695	thiamine biosynthesis protein (apbA) 36.9%
AF2412	thiamine biosynthesis protein (thiF) 60.2%	AF0088	thiamine biosynthesis protein, putative 28.2%
AF0553	thiamine biosynthesis protein (thiC) 38.1%	AF0702	thiamine biosynthetic enzyme (thi1) 50.0%
AF0702	thiamine biosynthesis protein, putative 28.2%	AF0733	thiamine monophosphate kinase (thiL) 30.4%
AF2073	thiamine phosphate pyrophosphorylase (thiE) 45.5%		
<i>Pyridine nucleotides</i>		AF1000	NH(3)-dependent NAD+ synthetase (nadE) 52.0%
AF1839	nicotinate-nucleotide pyrophosphorylase (nadC) 43.2%	AF1837	quinolinate synthetase (nadA), authentic frameshift 53.9%
<b>CELL ENVELOPE</b>		<i>Membranes, lipoproteins, and porins</i>	
<i>Membranes, lipoproteins, and porins</i>		AF1420	membrane protein 51.9%
AF1394	membrane protein, putative 32.8%	AF1394	membrane protein, putative 32.8%
<i>Surface polysaccharides, lipopolysaccharides and antigens</i>		AF0324	dTPD-glucose 4,6-dehydratase (rfbB) 50.0%
AF0043	first mannosyl transferase (wbaA-2) 30.0%	AF0906	first mannosyl transferase (wbaA-2) 29.0%
AF0906	first mannosyl transferase (wbaA-2) 29.0%	AF1728	GDP-D-mannose dehydratase (gmd-1), authentic frameshift 40.7%
AF0044	GDP-D-mannose dehydratase (gmd-1), authentic frameshift 40.7%	AF1142	glucose-1-phosphate cytidylyltransferase (rfbF) 38.6%
AF0424	glucose-1-phosphate thymidylyltransferase (graD-1) 27.7%	AF0325	glucose-1-phosphate thymidylyltransferase (graD-2) 45.2%
AF0321	glycosyl transferase 30.7%	AF0387	glycosyltransferase, putative 33.8%
AF0387	glycosyltransferase, putative 33.8%	AF0467	immunogenic protein (bcsp31-1) 34.7%
AF0635	immunogenic protein (bcsp31-2) 44.3%	AF0988	immunogenic protein (bcsp31-3) 26.3%
AF0632	LPS biosynthesis protein, putative 29.6%	AF0617	LPS biosynthesis protein, putative 29.0%
AF0617	LPS biosynthesis protein, putative 29.0%	AF0607	LPS glycosyltransferase, putative 29.7%
AF0326	mannose-1-phosphate guanylyltransferase (rfbM), authentic frameshift 42.4%	AF1097	mannose-6-phosphate isomerase/mannose-1-phosphate guanylyl transferase (manC) 43.1%
AF1097	mannose-6-phosphate isomerase/mannose-1-phosphate guanylyl transferase (manC) 43.1%	AF0035	mannosephosphate isomerase, putative 31.3%
AF0035	mannosephosphate isomerase, putative 31.3%	AF0045	mannosyltransferase A (mtfA) 38.7%
AF0045	mannosyltransferase A (mtfA) 38.7%	AF0458	phosphomannomutase (pmm) 30.6%
AF0458	ph		

AF1957	2-hydroxyglutaryl-CoA dehydratase, subunit beta (hgdB)	24.4%	AF0499	molybdopterin oxidoreductase, iron-sulfur binding subunit	41.5%	TCA cycle		
AF0130	acetylpolymine aminohydrolase (aphA)	38.7%	AF0500	molybdopterin oxidoreductase, membrane subunit	27.9%	AF1963	aconitase (acn)	571%
AF2290	acetylpolymine aminohydrolase, putative	33.3%	AF1202	molybdopterin oxidoreductase, iron-sulfur binding subunit	35.5%	AF1340	citrate synthase (citZ)	50.3%
AF0991	glutaryl-CoA dehydrogenase (gcdH)	48.7%	AF1203	molybdopterin oxidoreductase, molybdopterin binding subunit	30.1%	AF1098	fumarase (fum-1)	49.1%
AF1323	group II decarboxylase	28.0%	AF2384	molybdopterin oxidoreductase, molybdopterin binding subunit	34.6%	AF1099	fumarase (fum-2)	53.4%
AF2004	group II decarboxylase	46.1%	AF2385	molybdopterin oxidoreductase, iron-sulfur binding subunit	46.9%	AF0647	isocitrate dehydrogenase, NADP (icd)	57.2%
AF2295	group II decarboxylase	30.5%	AF2386	molybdopterin oxidoreductase, membrane subunit	30.3%	AF1727	malate oxidoreductase (mae)	52.3%
AF1665	ornithine cyclodeaminase (arcB)	35.3%	AF0159	molybdopterin oxidoreductase, molybdopterin binding subunit, putative	30.9%	AF0681	succinate dehydrogenase, flavoprotein subunit A (sdhA)	48.2%
<b>Anaerobic</b>								
AF1145	4-hydroxybutyrate CoA transferase (cat2-1)	46.5%	AF2267	NAD(P)H-flavin oxidoreductase	31.4%	AF0682	succinate dehydrogenase, iron-sulfur subunit B (sdhB)	51.3%
AF1854	4-hydroxybutyrate CoA transferase (cat2-2)	47.5%	AF0131	NAD(P)H-flavin oxidoreductase, putative	28.2%	AF0683	succinate dehydrogenase, subunit C (sdhC)	36.6%
AF0886	glycerol kinase (gpkK)	33.8%	AF2352	NADH dehydrogenase, subunit 1, putative	28.9%	AF0684	succinate dehydrogenase, subunit D (sdhD)	25.9%
AF1328	glycerol-3-phosphate dehydrogenase (gfpA)	27.8%	AF1828	NADH dehydrogenase, subunit 3	24.3%	AF1539	succinyl-CoA synthetase, alpha subunit (sucD-1)	56.9%
AF0871	glycerol-3-phosphate dehydrogenase (NAD(P)+) (gpsA)	36.3%	AF0248	NADH-dependent flavin oxidoreductase	36.7%	AF2185	succinyl-CoA synthetase, beta subunit (sucD-2)	63.5%
AF0020	L-carnitine dehydratase (caib-1)	31.3%	AF0342	nigerythrin, putative	33.3%	AF1540	succinyl-CoA synthetase, beta subunit (sucD-2)	51.3%
AF0990	L-carnitine dehydratase (caib-2)	31.2%	AF0546	nitrate reductase, gamma subunit (narI)	30.1%	AF2186	succinyl-CoA synthetase, beta subunit (sucC-2)	49.6%
<b>FATTY ACID AND PHOSPHOLIPID METABOLISM</b>								
<i>General</i>								
<b>ATP-proton motive force interconversion</b>								
AF1158	ATP synthase, subunit E, putative	47.1%	AF0832	nitrate reductase, gamma subunit, putative	29.3%	AF1736	3-hydroxy-3-methylglutaryl-coenzyme A reductase (mvaa)	571%
AF1161	H <sup>+</sup> -transporting ATP synthase, subunit A (atpA)	67.0%	AF1126	P450 cytochrome, putative	30.5%	AF0017	3-hydroxyacyl-CoA dehydrogenase (hbd-1)	41.1%
AF1167	H <sup>+</sup> -transporting ATP synthase, subunit B (atpB)	72.6%	AF0463	polyferredoxin (mvhB), authentic frameshift	32.2%	AF0285	3-hydroxyacyl-CoA dehydrogenase (hbd-2)	55.8%
AF1164	H <sup>+</sup> -transporting ATP synthase, subunit C (atpC)	37.5%	AF1379	quinone-reactive Ni/Fe-hydrogenase B-type cytochrome subunit (hycC)	29.0%	AF0434	3-hydroxyacyl-CoA dehydrogenase (hbd-3)	40.7%
AF1168	H <sup>+</sup> -transporting ATP synthase, subunit D (atpD)	47.1%	AF0173	reductase, assembly protein	30.0%	AF1025	3-hydroxyacyl-CoA dehydrogenase (hbd-4)	45.6%
AF1163	H <sup>+</sup> -transporting ATP synthase, subunit E (atpE)	36.3%	AF0547	reductase, iron-sulfur binding subunit	28.3%	AF1122	3-hydroxyacyl-CoA dehydrogenase (hbd-5)	45.2%
AF1165	H <sup>+</sup> -transporting ATP synthase, subunit F (atpF)	45.0%	AF0867	reductase, putative	33.3%	AF1177	3-hydroxyacyl-CoA dehydrogenase (hbd-6)	35.8%
AF1159	H <sup>+</sup> -transporting ATP synthase, subunit I (atpI)	30.1%	AF0880	rubredoxin (rd-1)	69.2%	AF1190	3-hydroxyacyl-CoA dehydrogenase (hbd-7)	46.5%
AF1160	H <sup>+</sup> -transporting ATP synthase, subunit K (atpK-1)	46.3%	AF1349	rubredoxin (rd-2)	67.9%	AF1206	3-hydroxyacyl-CoA dehydrogenase (hbd-8)	36.3%
AF1162	H <sup>+</sup> -transporting ATP synthase, subunit K (atpK-2)	46.3%	AF0832	rubryerythrin (rr1)	45.7%	AF2017	3-hydroxyacyl-CoA dehydrogenase (hbd-9)	35.4%
<b>Electron transport</b>								
AF2036	cytochrome C oxidase folding protein (coxD)	33.3%	AF0832	rubryerythrin (rr2)	63.7%	AF2273	3-hydroxyacyl-CoA dehydrogenase (hbd-10)	39.4%
AF0144	cytochrome C oxidase, subunit II (cbaB)	34.2%	AF1640	rubryerythrin (rr3)	37.8%	AF0018	3-ketoacyl-CoA thiolase (acaB-1)	41.0%
AF0142	cytochrome C oxidase, subunit II, putative	38.0%	AF2312	rubryerythrin (rr4)	41.4%	AF0034	3-ketoacyl-CoA thiolase (acaB-2)	38.3%
AF0190	cytochrome C oxidase, subunit II, putative	31.7%	AF0711	thioredoxin (trx-1)	28.4%	AF0133	3-ketoacyl-CoA thiolase (acaB-3)	32.3%
AF1057	cytochrome C-type biogenesis protein (ccdB)	30.7%	AF0769	thioredoxin (trx-2)	38.5%	AF0204	3-ketoacyl-CoA thiolase (acaB-5)	26.9%
AF2192	cytochrome C-type biogenesis protein (nirE)	36.1%	AF1284	thioredoxin (trx-3)	52.9%	AF0202	3-ketoacyl-CoA thiolase (acaB-6)	33.5%
AF2286	cytochrome oxidase, subunit I (cydA-1)	22.9%	AF2144	thioredoxin (trx-4)	48.9%	AF0283	3-ketoacyl-CoA thiolase (acaB-7)	42.0%
AF2297	cytochrome oxidase, subunit II (cydA-2)	31.5%	AF1339	ubiquinol-cytochrome C reductase complex, subunit VI requiring protein	60.9%	AF0438	3-ketoacyl-CoA thiolase (acaB-8)	42.4%
AF2046	cytochrome oxidase, subunit I, putative	25.1%				AF0967	3-ketoacyl-CoA thiolase (acaB-9)	33.7%
AF0528	cytochrome-c3 hydrogenase, subunit gamma	39.3%	<b>Fermentation</b>			AF0968	3-ketoacyl-CoA thiolase (acaB-10)	28.0%
AF0833	desulfoferredoxin (dfx)	63.0%	AF1779	2-hydroxyacyl dehydrogenase, putative	37.6%	AF1291	3-ketoacyl-CoA thiolase (acaB-11)	40.1%
AF0344	desulfoferredoxin, putative	47.3%	AF0469	2-ketoglutarate ferredoxin oxidoreductase, subunit alpha (korA)	52.3%	AF2416	3-ketoacyl-CoA thiolase (acaB-12)	49.9%
AF0287	electron transfer flavoprotein, subunit alpha (etfA)	39.7%	AF0468	2-ketoglutarate ferredoxin oxidoreductase, subunit beta (korB)	51.2%	AF1028	3-ketoacyl-CoA thiolase (acaB-13)	42.8%
AF0286	electron transfer flavoprotein, subunit beta (etfB)	38.8%	AF0470	2-ketoglutarate ferredoxin oxidoreductase, subunit delta (korD)	47.2%	AF1197	3-ketoacyl-CoA thiolase (fadA-1)	47.2%
AF1380	F420-nonreducing hydrogenase (vhtA)	34.8%	AF0471	2-ketoglutarate ferredoxin oxidoreductase, subunit gamma (korG)	40.0%	AF2243	3-ketoacyl-CoA thiolase (fadA-3)	40.3%
AF1371	F420-nonreducing hydrogenase (vhtD-1)	30.9%	AF2053	2-ketoisovalerate ferredoxin oxidoreductase, subunit alpha (vorA)	41.2%	AF0033	acyl carrier protein synthase (acaA-1)	28.6%
AF1378	F420-nonreducing hydrogenase (vhtD-2)	33.1%	AF2052	2-ketoisovalerate ferredoxin oxidoreductase, subunit beta (vorB)	42.7%	AF2415	acyl carrier protein synthase (acaA-2)	58.7%
AF1381	F420-nonreducing hydrogenase (vhtC)	46.1%	AF2054	2-ketoisovalerate ferredoxin oxidoreductase, subunit delta (vorD)	51.5%	AF0199	acyl-CoA dehydrogenase (acd-1)	35.9%
AF1824	F420H2:quinone oxidoreductase, 11.2 kDa subunit, putative	24.1%	AF2055	2-ketoisovalerate ferredoxin oxidoreductase, subunit gamma (vorE)	45.2%	AF0436	acyl-CoA dehydrogenase (acd-2)	44.1%
AF1823	F420H2:quinone oxidoreductase, 16.5 kDa subunit, putative	25.7%	AF0749	2-oxoacetyl ferredoxin oxidoreductase, subunit alpha (ora)	33.7%	AF0498	acyl-CoA dehydrogenase (acd-3)	22.9%
AF1832	F420H2:quinone oxidoreductase, 32 kDa subunit (nuoI)	95.5%	AF1286	acetyl-CoA synthetase (acs-1)	27.1%	AF0671	acyl-CoA dehydrogenase (acd-4)	37.9%
AF1833	F420H2:quinone oxidoreductase, 39 kDa subunit, putative	33.6%	AF1917	acetyl-CoA synthetase (acs-2)	47.3%	AF0845	acyl-CoA dehydrogenase (acd-5)	44.8%
AF1829	F420H2:quinone oxidoreductase, 39.7 kDa subunit, putative	43.8%	AF0677	acetyl-CoA synthetase (acs-3)	40.9%	AF0964	acyl-CoA dehydrogenase (acd-6)	35.8%
AF1831	F420H2:quinone oxidoreductase, 41.2 kDa subunit, putative	34.8%	AF0975	acetyl-CoA synthetase (acs-4)	42.3%	AF1026	acyl-CoA dehydrogenase (acd-7)	42.6%
AF1827	F420H2:quinone oxidoreductase, 43.2 kDa subunit, putative	26.9%	AF0976	acetyl-CoA synthetase (acs-5)	36.2%	AF1141	acyl-CoA dehydrogenase (acd-8)	43.2%
AF1830	F420H2:quinone oxidoreductase, 45 kDa subunit (nuoD)	80.0%	AF1287	acetyl-CoA synthetase (acs-6)	34.3%	AF1293	acyl-CoA dehydrogenase (acd-9)	45.8%
AF1825	F420H2:quinone oxidoreductase, 53.9 kDa subunit (nuoM)	32.1%	AF0024	alcohol dehydrogenase, iron-containing	38.2%	AF2057	acyl-CoA dehydrogenase (acd-10)	44.6%
AF1826	F420H2:quinone oxidoreductase, 72.4 kDa subunit (nuoL)	33.2%	AF0339	alcohol dehydrogenase, iron-containing	37.4%	AF2244	acyl-CoA dehydrogenase (acd-11)	42.6%
AF0156	ferredoxin (fdx-1)	45.3%	AF2019	alcohol dehydrogenase, iron-containing	35.7%	AF2275	acyl-CoA dehydrogenase (acd-12)	38.9%
AF0166	ferredoxin (fdx-2)	49.2%	AF2389-C	acetyl-CoA synthetase, putative	64.8%	AF1175	acyl-CoA dehydrogenase, short chain-specific (acdS)	30.1%
AF0332	ferredoxin (fdx-3)	53.2%	AF2389-N	acetyl-CoA synthetase, putative	59.3%	AF0818	acylphosphatase (acyP)	36.8%
AF0427	ferredoxin (fdx-4)	56.1%	AF2101	alcohol dehydrogenase, zinc-dependent	34.8%	AF0968	alkylidihydroxyacetonephosphate synthase	33.6%
AF0923	ferredoxin (fdx-5)	56.9%	AF2102	aldehyde ferredoxin oxidoreductase (aor-1)	41.1%	AF2286	bifunctional short chain isoprenyl phosphate synthase (idsA)	42.7%
AF1010	ferredoxin (fdx-6)	44.4%	AF0077	aldehyde ferredoxin oxidoreductase (aor-2)	32.6%	AF0220	biotin carboxylase (acc)	53.1%
AF1239	ferredoxin (fdx-7)	29.0%	AF0340	aldehyde ferredoxin oxidoreductase (aor-3)	38.4%	AF0865	carboxylesterase (est-1)	27.1%
AF2142	ferredoxin (fdx-8)	38.0%	AF2281	aldehyde ferredoxin oxidoreductase (aor-4)	53.0%	AF1537	carboxylesterase (est-2)	29.0%
AF0164	ferredoxin-nitrite reductase (nirA)	29.7%	AF0006	cornioid methyltransferase protein (mtaC-1)	30.7%	AF2336	carboxylesterase (est-3)	30.4%
AF2332	flavodoxin, putative	30.3%	AF0007	cornioid methyltransferase protein (mtaC-2)	25.5%	AF1716	carboxylesterase (estA)	40.4%
AF0167	flavoprotein (fprA-1)	33.2%	AF0394	D-formate dehydrogenase, cytochrome-type (did)	31.9%	AF1744	CDP-diacylglycerol-glycerol-3-phosphate 3-phosphatidyltransferase (pgsA-2)	26.7%
AF1520	flavoprotein (fprA-2)	47.2%	AF0560	formate dehydrogenase (fdhH), authentic frameshift	32.9%	AF1143	CDP-diacylglycerol-glycerol-3-phosphate-3-phosphatidyltransferase (pgsA-1)	27.0%
AF0257	fumarate reductase, flavoprotein subunit (fdrA)	27.0%	AF1199	glutacinate CoA-transferase, subunit A (gctA)	31.9%	AF2044	CDP-diacylglycerol-serine O-phosphatidyltransferase (pssa)	36.6%
AF1483	glutaredoxin (grx-1)	34.3%	AF1198	glutacinate CoA-transferase, subunit B (gctB)	37.0%	AF0435	enoyl-CoA hydratase (fad-1)	47.6%
AF2145	glutaredoxin (grx-2)	38.8%	AF1489	independent ferredoxin oxidoreductase, authentic frameshift	48.1%	AF0885	enoyl-CoA hydratase (fad-2)	39.9%
AF0663	heterodisulfide reductase, subunit A (hdrA-1)	42.2%	AF2030	independent ferredoxin oxidoreductase, subunit alpha (iorA)	48.1%	AF0963	enoyl-CoA hydratase (fad-3)	48.6%
AF1377	heterodisulfide reductase, subunit A (hdrA-2)	46.8%	AF0807	L-lactate dehydrogenase, cytochrome-type (lldD)	41.1%	AF1641	enoyl-CoA hydratase (fad-4)	41.7%
AF0662	heterodisulfide reductase, subunit A / methylyliologen reducing hydrogenase, subunit delta	34.2%	AF0885	L-malate dehydrogenase, NAD <sup>+</sup> -dependent (mdtA)	40.1%	AF2429	enoyl-CoA hydratase (fad-5)	34.7%
AF1238	heterodisulfide reductase, subunit A / methylyliologen reducing hydrogenase, subunit delta	53.7%	AF2085	oxaloacetate decarboxylase, biotin carboxyl carrier subunit, putative	38.7%	AF1763	lipase, putative	33.5%
AF1375	heterodisulfide reductase, subunit B (hdrB)	36.0%	AF2084	oxaloacetate decarboxylase, sodium ion pump subunit (oadB)	59.8%	AF0089	long-chain-fatty-acyl-CoA ligase (fadD-1)	31.9%
AF0271	heterodisulfide reductase, subunit C (hdrC)	35.3%	AF1252	oxaloacetate decarboxylase, subunit alpha (oadA)	63.3%	AF0200	long-chain-fatty-acyl-CoA ligase (fadD-2)	34.8%
AF0502	heterodisulfide reductase, subunit D, putative	33.8%	AF1701	pyruvate ferredoxin oxidoreductase, subunit alpha (porA)	50.3%	AF0687	long-chain-fatty-acyl-CoA ligase (fadD-3)	31.1%
AF0809	heterodisulfide reductase, subunit D, putative	100.0%	AF1702	pyruvate ferredoxin oxidoreductase, subunit beta (porB)	50.7%	AF0840	long-chain-fatty-acyl-CoA ligase (fadD-4)	38.1%
AF0661	heterodisulfide reductase, subunit E, putative	23.8%	AF1700	pyruvate ferredoxin oxidoreductase, subunit delta (porD)	53.1%	AF1029	long-chain-fatty-acyl-CoA ligase (fadD-5)	37.8%
AF0755	heterodisulfide reductase, subunit E and D, putative	31.8%	AF1699	pyruvate ferredoxin oxidoreductase, subunit gamma (porG)	50.9%	AF1610	long-chain-fatty-acyl-CoA ligase (fadD-6)	36.0%
AF0056	iron-sulfur binding reductase	38.5%	<b>Gluconeogenesis</b>			AF1772	long-chain-fatty-acyl-CoA ligase (fadD-7)	38.7%
AF1773	iron-sulfur binding reductase	33.3%	AF0710	phosphoenolpyruvate synthase (ppsA)	61.4%	AF1932	long-chain-fatty-acyl-CoA ligase (fadD-8)	31.0%
AF1998	iron-sulfur binding reductase	29.6%	AF1146	3-phosphoglycerate kinase (pgk)	48.8%	AF2368	long-chain-fatty-acyl-CoA ligase (fadD-9)	38.7%
AF0627	iron-sulfur cluster binding protein	45.5%	AF1132	enolase (eno)	53.9%	AF1753	lysophospholipase	33.5%
AF0688	iron-sulfur cluster binding protein	44.8%	AF1732	glyceraldhyde 3-phosphate dehydrogenase (gap)	56.6%	AF0196	medium-chain acyl-CoA ligase (alkK-1)	34.6%
AF1153	iron-sulfur cluster binding protein	27.9%	AF1304	triosephosphate isomerase (tpiA)	56.4%	AF0262	medium-chain acyl-CoA ligase (alkK-2)	38.6%
AF1185	iron-sulfur cluster binding protein	36.7%	<b>Glycolysis</b>			AF0672	medium-chain acyl-CoA ligase (alkK-3)	31.0%
AF1263	iron-sulfur cluster binding protein	42.1%	AF1461	iron-sulfur cluster binding protein, putative	51.0%	AF1261	medium-chain acyl-CoA ligase (alkK-4)	42.7%
AF2380	iron-sulfur cluster binding protein	36.3%	AF1436	iron-sulfur flavoprotein (isf-1)	57.9%	AF2033	medium-chain acyl-CoA ligase (alkK-5)	33.5%
AF2381	iron-sulfur cluster binding protein	34.4%	AF1519	iron-sulfur flavoprotein (isf-2)	56.6%	AF2289	mevalonate kinase (mvk)	40.8%
AF2409	iron-sulfur cluster binding protein	28.2%	AF1896	iron-sulfur flavoprotein (isf-3)	37.1%	AF1794	myo-inositol-1-phosphate synthase (ino1)	42.2%
AF0076	iron-sulfur cluster binding protein	32.7%	AF1372	methylglucosyl-reducing hydrogenase, subunit alpha (vhuA)	39.4%	AF2045	phosphatidylserine decarboxylase (psd2)	42.5%
AF1461	iron-sulfur cluster binding protein, putative	51.0%	AF1374	methylglucosyl-reducing hydrogenase, subunit delta (vhuD)	41.7%	AF1674	sn-glycerol-1-phosphate dehydrogenase (gldA)	44.0%
AF1436	iron-sulfur flavoprotein (isf-1)	57.9%	AF0157	molybdopterin oxidoreductase, iron-sulfur binding subunit	38.6%	<b>AUTOTROPHIC METABOLISM</b>		
AF1519	iron-sulfur flavoprotein (isf-2)	56.6%	AF0174	molybdopterin oxidoreductase, membrane subunit	26.0%	<i>General</i>		
AF1896	iron-sulfur flavoprotein (isf-3)	37.1%	AF0175	molybdopterin oxidoreductase, iron-sulfur binding subunit	42.0%	AF1100	acetyl-CoA decarboxylase/synthase, subunit alpha (cdhA-1)	50.4%
AF1372	methylglucosyl-reducing hydrogenase, subunit alpha (vhuA)	39.4%	AF0176	molybdopterin oxidoreductase, molybdopterin binding subunit	42.0%	AF2397	acetyl-CoA decarboxylase/synthase, subunit alpha (cdhA-2)	54.0%
AF1374	methylglucosyl-reducing hydrogenase, subunit delta (vhuD)	41.7%						

AF1935	N5,N10-methylenetetrahydromethanopterin cyclohydrolase (mch)	97.3%	AF0004	RNase I inhibitor	54.5%	AF0633	isoleucyl-tRNA synthetase (IleS)	48.9%
AF0714	N5,N10-methylenetetrahydromethanopterin dehydrogenase (mtd)	61.8%	AF0021	signal-transducing histidine kinase	26.1%	AF2421	leucyl-tRNA synthetase (LeuS)	49.7%
AF1066	N5,N10-methylenetetrahydromethanopterin reductase (mer-1)	59.1%	AF0208	signal-transducing histidine kinase	27.9%	AF1216	lysyl-tRNA synthetase (LysS)	43.6%
AF1196	N5,N10-methylenetetrahydromethanopterin reductase (mer-2)	37.4%	AF0450	signal-transducing histidine kinase	32.4%	AF1453	methionyl-tRNA synthetase (MetS)	45.2%
AF0009	N5-methyltetrahydromethanopterin:coenzyme M methyltransferase (mtr)	42.1%	AF0770	signal-transducing histidine kinase	26.9%	AF1955	phenylalanyl-tRNA synthetase, subunit alpha (pheS)	44.4%
AF1587	ribulose biphosphate carboxylase, large subunit (rbcL-1)	40.6%	AF0893	signal-transducing histidine kinase	28.7%	AF1424	phenylalanyl-tRNA synthetase, subunit beta (pheT)	42.6%
AF1638	ribulose biphosphate carboxylase, large subunit (rbcL-2)	44.9%	AF1184	signal-transducing histidine kinase	29.8%	AF1609	prolyl-tRNA synthetase (ProS)	56.8%
AF1930	tungsten formylmethanofuran dehydrogenase, subunit A (fwdA)	48.9%	AF1482	signal-transducing histidine kinase	28.5%	AF2035	seryl-tRNA synthetase (SerS)	45.4%
AF1650	tungsten formylmethanofuran dehydrogenase, subunit B (fwdB-1)	37.0%	AF1467	signal-transducing histidine kinase	37.4%	AF0548	threonyl-tRNA synthetase (ThrS)	46.3%
AF1929	tungsten formylmethanofuran dehydrogenase, subunit B (fwdB-2)	49.4%	AF1472	signal-transducing histidine kinase	20.4%	AF1694	tryptophanyl-tRNA synthetase (TrpS)	52.4%
AF1931	tungsten formylmethanofuran dehydrogenase, subunit C (fwdC)	44.1%	AF1483	signal-transducing histidine kinase	27.7%	AF0776	tyrosyl-tRNA synthetase (TyrS)	57.6%
AF1651	tungsten formylmethanofuran dehydrogenase, subunit D (fwdD-1)	32.6%	AF1515	signal-transducing histidine kinase	32.0%	AF2224	valyl-tRNA synthetase (ValS)	54.5%
AF1928	tungsten formylmethanofuran dehydrogenase, subunit D (fwdD-2)	52.6%	AF1639	signal-transducing histidine kinase	29.9%	<i>Degradation of proteins, peptides, and glycopeptides</i>		
AF0177	tungsten formylmethanofuran dehydrogenase, subunit E (fwdE)	29.7%	AF1721	signal-transducing histidine kinase	34.5%	AF1976	26S protease regulatory subunit 4	66.0%
AF1644	tungsten formylmethanofuran dehydrogenase, subunit F (fwdF)	38.2%	AF1209	signal-transducing histidine kinase	31.6%	AF1653	alkaline serine protease (sprM)	44.5%
AF1649	tungsten formylmethanofuran dehydrogenase, subunit G (fwdG)	45.6%	AF0881	signal-transducing histidine kinase, authentic frameshift	26.5%	AF0578	aminopeptidase, putative	27.9%
<b>PURINES, PYRIMIDINES, NUCLEOSIDES, AND NUCLEOTIDES</b>								
<i>2'-Deoxyribonucleotide metabolism</i>								
AF1108	deoxycytidine triphosphate deaminase, putative	38.1%	AF0277	signal-transducing histidine kinase, putative	29.8%	AF0364	ATP-dependent protease La (lon)	36.6%
AF1664	ribonucleotide reductase (nrd)	59.7%	AF0410	signal-transducing histidine kinase, putative	27.1%	AF1946	cysteine proteinase, putative	36.2%
AF1554	thioredoxin reductase (trxB)	45.2%	AF0448	signal-transducing histidine kinase, putative	26.1%	AF1281	intracellular protease (pilP)	56.0%
AF2047	thymidylate synthase, putative	33.1%	AF0584	signal-transducing histidine kinase, putative	25.2%	AF1112	O-sialoglycoprotein endopeptidase (gcp)	57.6%
<i>Nucleotide and nucleoside interconversions</i>								
AF0676	5'-nucleotidase (ntf)	30.9%	AF2022	signal-transducing histidine kinase, putative	22.0%	AF0665	O-sialoglycoprotein endopeptidase, putative	35.8%
AF0676	adenylate kinase (adeK)	56.1%	AF2420	signal-transducing histidine kinase, putative	28.4%	AF2086	protease inhibitor, putative	37.0%
AF1900	cytidylate kinase (cmk)	48.6%	AF0442	succinoylcan biosynthesis regulator (exsB)	37.2%	AF0490	proteasome, subunit alpha (psmA)	60.8%
AF0767	nucleoside diphosphate kinase (ndk)	56.4%	AF1516	sugar fermentation stimulation protein (sfsA)	31.0%	AF0481	proteasome, subunit beta (psmB)	58.3%
AF0061	thymidylate kinase (tmk)	34.9%	AF1270	transcriptional regulatory protein, ArsR family	35.4%	AF2034	X-pro aminopeptidase (pepQ)	34.6%
AF1308	thymidylate kinase, putative	26.3%	AF1544	transcriptional regulatory protein, ArsR family	32.3%	<i>Protein modification</i>		
AF2042	uridylate kinase (pyrH)	53.6%	AF1853	transcriptional regulatory protein, ArsR family	34.9%	AF0656	antibiotic maturation protein (pmbA)	32.7%
<i>Purine ribonucleotide biosynthesis</i>								
AF2242	adenylosuccinate lyase (purB)	52.3%	AF2136	transcriptional regulatory protein, ArsR family	39.8%	AF0378	CODH nickel-insertion accessory protein (cocC-1)	35.7%
AF0841	adenylosuccinate synthetase (purA)	70.8%	AF0439	transcriptional regulatory protein, AsnC family	29.8%	AF1685	CODH nickel-insertion accessory protein (cocC-2)	47.4%
AF0873	amidophosphoribosyltransferase (purF)	55.8%	AF0474	transcriptional regulatory protein, AsnC family	51.0%	AF1615	cofactor modifying protein (cmo)	27.2%
AF0253	GMP synthase (guaA-1)	59.8%	AF0584	transcriptional regulatory protein, AsnC family	35.3%	AF2195	deoxyhypusine synthase (dys1-1)	32.6%
AF1320	GMP synthase (guaA-2)	49.4%	AF1121	transcriptional regulatory protein, AsnC family	35.8%	AF0381	diphthine synthase (dph5)	40.8%
AF1911	inosine monophosphate cyclohydrolase	36.3%	AF1448	transcriptional regulatory protein, AsnC family	30.6%	AF2324	fmu and fmv protein	40.0%
AF0847	inosine monophosphate dehydrogenase (guaB-1)	41.6%	AF1723	transcriptional regulatory protein, AsnC family	46.4%	AF1367	hydrogenase expression/formation protein (hypA)	40.4%
AF2118	inosine monophosphate dehydrogenase (guaB-2)	31.9%	AF1743	transcriptional regulatory protein, AsnC family	34.9%	AF1388	hydrogenase expression/formation protein (hypB)	54.4%
AF1259	inosine monophosphate dehydrogenase, putative	51.6%	AF2127	transcriptional regulatory protein, LysR family	30.8%	AF1369	hydrogenase expression/formation protein (hypC)	40.5%
AF1157	phosphoribosylamino-glycine lyase (purD)	40.9%	AF0114	transcriptional regulatory protein, putative	35.6%	AF1370	hydrogenase expression/formation protein (hypD)	46.0%
AF1271	phosphoribosylaminoimidazole carboxylase (purE)	42.8%	AF1988	transcriptional regulatory protein, Rok family	32.9%	AF1365	hydrogenase expression/formation protein (hypE)	51.5%
AF1272	phosphoribosylaminoimidazole succinocarboxamide synthase (purC)	34.7%	AF1012	transcriptional regulatory protein, Sir2 family	38.9%	AF1366	hydrogenase expression/formation regulatory protein (hypF)	45.1%
AF1693	phosphoribosylformylglycinamide cyclo-lyase (purM)	53.8%	AF1676	transcriptional regulatory protein, Sir2 family	40.6%	AF0036	L-isocapsaryl protein carboxyl methyltransferase (pcm-1)	60.7%
AF1260	phosphoribosylformylglycinamide synthase I (purC)	40.9%	AF1817	transcriptional regulatory protein, TetR family	24.5%	AF2322	L-isocapsaryl protein carboxyl methyltransferase (pcm-2)	59.3%
AF1940	phosphoribosylformylglycinamide synthase II (purL)	41.5%	AF0363	transcriptional repressor (cinR)	27.5%	AF1840	methionyl aminopeptidase (map)	48.6%
AF0589	ribose-phosphate pyrophosphokinase (prsA-1)	32.0%	<b>REPLICATION</b>			AF1840	peptidyl-prolyl cis-trans isomerase (slyD)	34.4%
AF1419	ribose-phosphate pyrophosphokinase (prsA-2)	41.1%	<i>DNA replication, restriction, modification, recombination, and repair</i>			AF0653	proliferating-cell nuclear antigen P120, putative	35.7%
<i>Pyrimidine ribonucleotide biosynthesis</i>								
AF0106	aspartate carbamoyltransferase, catalytic subunit (pyrB)	60.7%	AF2117	3-methyladenine DNA glycosylase (alkA)	30.0%	AF2039	proliferating-cell nuclear antigen P120, putative	44.2%
AF0107	aspartate carbamoyltransferase, regulatory subunit (pyrI)	48.2%	AF1195	activator 1, replication factor C, 53 kDa subunit	43.7%	AF1449	pyruvate formate-lyase 2 (pflD)	37.8%
AF1274	carbamoyl-phosphate synthase, large subunit (carB)	65.1%	AF0465	DNA gyrase, subunit A (gyrA)	48.4%	AF1450	pyruvate formate-lyase 2 activating enzyme (pflC)	38.8%
AF1273	carbamoyl-phosphate synthase, small subunit (carA)	55.2%	AF0530	DNA gyrase, subunit B (gyrB)	58.4%	AF0117	pyruvate formate-lyase activating enzyme (act-1)	25.5%
AF0252	CTP synthase (pyrG)	58.3%	AF1388	DNA helicase, putative	46.8%	AF0918	pyruvate formate-lyase activating enzyme (act-2)	42.3%
AF2250	dihydroorotase (pyrC)	37.2%	AF0623	DNA ligase (lig)	32.7%	AF2278	pyruvate formate-lyase activating enzyme (act-3)	42.5%
AF0745	dihydroorotase dehydrogenase (pyrD)	44.8%	AF1725	DNA ligase, putative	32.7%	AF1961	pyruvate formate-lyase activating enzyme (pflX)	50.2%
AF1741	orate phosphoribosyl transferase (pyrE)	49.0%	AF0497	DNA polymerase B1 (polB)	45.1%	AF0380	transmembrane oligosaccharyl transferase, putative	27.8%
AF0386	orate phosphoribosyl transferase, putative	39.0%	AF0693	DNA polymerase B2 (boxA), authentic frameshift	32.3%	AF0329	transmembrane oligosaccharyl transferase, putative	29.3%
<i>Salvage of nucleosides and nucleotides</i>								
AF0240	adenine deaminase (adeC)	39.5%	AF0972	DNA polymerase III, subunit epsilon (dnaQ)	31.9%	<i>Ribosomal proteins: synthesis and modification</i>		
AF1764	dCMP deaminase, putative	39.0%	AF2277	DNA polymerase, bacteriophage-typing	36.9%	AF1490	LSU ribosomal protein L1P (rpl1P)	48.6%
AF1788	methylthioadenosine phosphorylase (mtaP)	40.0%	AF0742	DNA primase, putative	26.8%	AF1922	LSU ribosomal protein L2P (rpl2P)	60.4%
AF1341	thymidine phosphorylase (deoA-1)	46.7%	AF0264	DNA repair protein RAD2 (rad2)	44.4%	AF1925	LSU ribosomal protein L3P (rpl3P)	56.5%
AF1342	thymidine phosphorylase (deoA-2)	40.7%	AF0358	DNA repair protein RAD25	32.5%	AF1924	LSU ribosomal protein L4P (rpl4P)	56.4%
AF0239	xanthine-guanine phosphoribosyltransferase (gptA-1)	25.7%	AF1031	DNA repair protein RAD32 (rad32)	37.6%	AF1912	LSU ribosomal protein L5P (rpl5P)	51.7%
AF1789	xanthine-guanine phosphoribosyltransferase (gptA-2)	28.2%	AF1940	DNA repair protein RAD51 (radA)	59.3%	AF1909	LSU ribosomal protein L6P (rpl6P)	53.7%
<b>REGULATORY FUNCTIONS</b>								
AF1959	(R)-hydroxylglutaryl-CoA dehydratase activator (hdgC)	51.2%	AF2096	DNA repair protein REC	40.0%	AF0764	LSU ribosomal protein L7AE (rpl7AE)	60.7%
AF0168	arsenical resistance operon repressor, putative	36.7%	AF2418	DNA repair protein, putative	28.9%	AF1491	LSU ribosomal protein L10E (rpl10E)	45.6%
AF2204	arylsulfatase regulatory protein, putative	29.9%	AF1806	DNA topoisomerase I (topA)	36.2%	AF0538	LSU ribosomal protein L11P (rpl11P)	67.8%
AF0074	biotin operon repressor/biotin-[acetyl CoA carboxylase] ligase (birA)	36.6%	AF0940	DNA topoisomerase VI, subunit A (top6A)	39.8%	AF1492	LSU ribosomal protein L12A (rpl12A)	76.0%
AF1724	dinitrogenase reductase activating glycohydrolase (dntG)	37.9%	AF0652	DNA topoisomerase VI, subunit B (top6B)	43.9%	AF1128	LSU ribosomal protein L13P (rpl13P)	47.4%
AF2232	ferric uptake regulation protein (fur)	25.8%	AF1692	endonuclease III (ntf)	44.3%	AF1915	LSU ribosomal protein L14P (rpl14P)	65.7%
AF1785	iron-dependent repressor	42.0%	AF0580	exodeoxyribonuclease III (kthA)	41.3%	AF2319	LSU ribosomal protein L15E (rpl15E)	70.3%
AF2395	iron-dependent repressor	40.0%	AF2314	methylated-DNA-protein-cysteine methyltransferase (ogt)	55.3%	AF1903	LSU ribosomal protein L15P (rpl15P)	53.8%
AF0245	iron-dependent repressor (desR)	28.2%	AF1409	modification methylase, type III R/M system	31.4%	AF1127	LSU ribosomal protein L18E (rpl18E)	53.8%
AF1984	iron-dependent repressor (trpR)	28.3%	AF1234	mutator protein MutT (mutT)	63.8%	AF1906	LSU ribosomal protein L18P (rpl18P)	57.8%
AF2430	lacZ expression regulatory protein (ccp)	29.6%	AF2200	mutator protein MutU, putative	42.0%	AF1907	LSU ribosomal protein L19E (rpl19E)	55.5%
AF1622	leucine responsive regulatory protein (lrp)	29.1%	AF0335	proliferating-cell nuclear antigen (pou3)	33.7%	AF1529	LSU ribosomal protein L21E (rpl21E)	53.2%
AF0673	mercuric resistance operon regulatory protein (merR)	37.6%	AF0694	replication control protein A, putative	30.2%	AF1920	LSU ribosomal protein L22P (rpl22P)	55.2%
AF2425	methanol dehydrogenase regulatory protein (mxoR)	48.3%	AF1024	reverse gyrase (topR)	40.7%	AF1923	LSU ribosomal protein L23P (rpl23P)	55.6%
AF1475	mitochondrial benzodiazepine receptor/sensory transduction protein	38.4%	AF0621	ribonuclease HI (rnhB)	39.3%	AF0537	LSU ribosomal protein L24A (rpl24A)	51.4%
AF0198	monoamine oxidase regulatory protein, putative	41.7%	AF1715	type I restriction-modification enzyme, M subunit, authentic frameshift	63.0%	AF0766	LSU ribosomal protein L24E (rpl24E)	62.1%
AF1933	monoamine oxidase regulatory protein, putative	38.9%	AF1708	type I restriction-modification enzyme, R subunit	38.2%	AF1914	LSU ribosomal protein L24F (rpl24F)	57.8%
AF0978	nitrogen regulatory protein P-II (glnB-1)	61.7%	AF1710	type I restriction-modification enzyme, S subunit	33.0%	AF1918	LSU ribosomal protein L29P (rpl29P)	44.6%
AF1747	nitrogen regulatory protein P-II (glnB-2)	58.0%	<b>TRANSCRIPTION</b>			AF1890	LSU ribosomal protein L30E (rpl30E)	41.7%
AF1750	nitrogen regulatory protein P-II (glnB-3)	60.7%	<i>DNA-dependent RNA polymerase</i>			AF1904	LSU ribosomal protein L30P (rpl30P)	55.9%
AF0331	pheromone shutdown protein (trab)	40.5%	AF1888	DNA-directed RNA polymerase, subunit A' (rpoA1)	63.6%	AF2066	LSU ribosomal protein L31E (rpl31E)	50.6%
AF1797	phosphate regulatory protein, putative	30.7%	AF1889	DNA-directed RNA polymerase, subunit A'' (rpoA2)	55.7%	AF1908	LSU ribosomal protein L32E (rpl32E)	51.2%
AF0521	protease synthase and sporulation regulator Pa1, putative	52.4%	AF1887	DNA-directed RNA polymerase, subunit B' (rpoB1)	65.3%	AF0057	LSU ribosomal protein L37AE (rpl37AE)	47.6%
AF1627	repressor protein	59.1%	AF1886	DNA-directed RNA polymerase, subunit B'' (rpoB2)	57.1%	AF0874	LSU ribosomal protein L37E (rpl37E)	57.9%
AF1793	repressor protein	54.5%	AF2282	DNA-directed RNA polymerase, subunit D (rpoD)	34.6%	AF2067	LSU ribosomal protein L39E (rpl39E)	56.9%
AF0449	response regulator	38.1%	AF1117	DNA-directed RNA polymerase, subunit E' (rpoE1)	48.4%	AF1430	LSU ribosomal protein L40E (rpl40E)	73.3%
AF1063	response regulator	36.3%	AF1116	DNA-directed RNA polymerase, subunit E'' (rpoE2)	40.0%	AF1915	LSU ribosomal protein L44E (rpl44E)	43.8%
AF1256	response regulator	42.5%	AF1885	DNA-directed RNA polymerase, subunit H (rhoH)	59.5%	AF2064	LSU ribosomal protein LXX (rplXXA)	53.5%
AF1384	response regulator	44.7%	AF1131	DNA-directed RNA polymerase, subunit K (rhoK)	61.9%	AF0739	ribosomal protein S18 alanine acetyltransferase	38.5%
AF1473	response regulator	32.5%	AF0207	DNA-directed RNA polymerase, subunit L (rhoL)	42.0%	AF2303	ribosomal protein S6 modification protein (rimK)	32.2%
AF1898	response regulator	48.7%	AF1130	DNA-directed RNA polymerase, subunit N (rhoN)	58.8%	AF1133	SSU ribosomal protein S2P (rps2P)	58.3%
AF2249	response regulator	44.8%	<i>Transcription factors</i>			AF1919	SSU ribosomal protein S3P (rps3P)	50.0%
AF2419	response regulator	37.9%	AF1813	TBP-interacting protein TIP49	45.7%	AF1913	SSU ribosomal protein S4E (rps4E)	48.9%
<i>RNA processing</i>								
<i>Amino acyl tRNA synthetases</i>								
AF1783	dimethyladenosine transferase (ksgA)	44.7%	AF1299	transcription initiation factor IIB	60.4%	AF2284	SSU ribosomal protein S4P (rps4P)	59.1%
AF0694	arginyl-tRNA synthetase (argS)	48.8%	AF0373	transcription initiation factor IID	59.4%	AF1905	SSU ribosomal protein S5P (rps5P)	60.0%
AF0920	aspartyl-tRNA synthetase (aspS)	62.5%	AF0757	transcription initiation factor IIE, subunit alpha, putative	23.5%	AF0611	SSU ribosomal protein S6E (rps6E)	50.8%
AF0411	cysteinyl-tRNA synthetase (cysS)	46.1%	AF1891	transcription termination-antitermination factor NusA, putative	48.9%	AF1893	SSU ribosomal protein S7P (rps7P)	59.6%
AF0280	glutamyl-tRNA synthetase (gltX)	44.9%	AF1235	transcription termination-antitermination factor NusA, putative	48.9%	AF2152	SSU ribosomal protein S8E (rps8E)	61.6%
AF0916	glycyl-tRNA synthetase (glsS)	51.2%	AF1235	transcription termination-antitermination factor NusA, putative	48.9%	AF1912	SSU ribosomal protein S8P (rps8P)	64.8%
AF1642	histidyl-tRNA synthetase (hisS)	46.0%	AF1235	transcription-associated protein TFIIS	59.0%	AF1129	SSU ribosomal protein S	

